Global pathfollowing of homoclinic orbits in two-parameter flows

Bernold Fiedler
Mathematisches Institut A
Universität Stuttgart
Pfaffenwaldring 57
D - 7000 Stuttgart

August 26, 1992
revised December 6, 1995

Abstract

The main goal of this paper is a global continuation theorem for homoclinic solutions of autonomous ordinary differential equations with two real parameters. In one-parameter flows, Hopf bifurcation serves as a starting point for global paths of periodic orbits. B-points, alias Arnol'd-Bogdanov-Takens points, play an analogous role for paths of homoclinic orbits in two-parameter flows. In fact, a path of homoclinic orbits emanating from a B-point can be continued in phase space until it terminates at another B-point, or becomes unbounded, or approaches a region with chaotic dynamics.

This result is obtained via a new topological invariant for homoclinic orbits, based on approximation of the homoclinic orbit by nearby periodic orbits. Several local bifurcation results for homoclinic and heteroclinic orbits are reviewed, along the way, to illustrate scope, significance, and limitations of the global approach. The paper concludes with an extensive discussion, including "non-generic" aspects like equivariance, Hamiltonian and reversible systems, and topics like numerical continuation, and partial differential equations.

Contents

1 Introduction **1**

2 Basic examples and definitions **4**

2.1 Example: B-point 4

2.2 Example: one-parameter homoclinics 6

2.3 Definition: tame, chaotic 8

2.4 Definition: generic 9

2.5 Proposition 10

2.6 Definition: ϵ-length 12

2.7 Example: fold-Hopf 12

2.8 Proposition: loops 16

2.9 Example: resonant homoclinic 17

2.10 Example: Tresser's tame 8, saddle focus 20

2.11 Definition: stratified 22

3 Global continuation **25**

3.1 Definition: orientation of tame paths 26

3.2 Definition: B-index 27

3.3 Lemma 27

3.4 Theorem 33

3.5 Remarks 34

4 Proof **36**

4.1 Lemma 38

5 More examples **44**

5.1 Example: fold hitting 44

5.2 Example: bi-contractive het loop 47

5.3 Example: codimension three unfoldings 50

5.4 Example: Belyakov transitions 54

5.5 Example: the fold-Hopf, revisited 55

5.6 Example: Bykov's semi-robust het loop 56

5.7 Example: tame 8, doubly twisted real saddle 58

5.8 Example: tame butterfly, real saddle 61

6 Homoclinic trapping **64**

6.1 Example: trapped lip 64

6.2 Example: dissipative trapping 67

7 Discussion **70**

References **85**

1 Introduction

A *heteroclinic orbit* of a flow is by definition a solution $x = h(t)$, $t \in \mathbb{R}$, of a differential equation

$$\dot{x} = f(\lambda, x), \quad x \in X = \mathbb{R}^N \tag{1.1}$$

with or without parameters λ, such that $h(t)$ converges for both $t \to +\infty$ and $t \to -\infty$,

$$A_\pm := \lim_{t \to \pm\infty} h(t), \quad A_+ \neq A_-. \tag{1.2}$$

The limits are equilibria of (1.1), by invariance of ω-limit sets. If $A_+ = A_-$, then $h(t)$ is called a *homoclinic orbit*. In either case, we call $A_\pm$ the *associated equilibria* of the (homoclinic or heteroclinic) orbit $h(t)$. See figure 1.1. Technically speaking, if $A_\pm$ are hyperbolic equilibria, then homoclinic or heteroclinic orbits arise as nontrivial intersections of the respective unstable and stable manifolds

$$W^u(A_-) \cap W^s(A_+).$$

See, for example, [Chow & Hale] (1982), [Arnol'd] (1992), [Guckenheimer & Holmes] (1990), [Wiggins] (1988) for a general background.

From an applied point of view, homoclinic orbits serve as one possible cause of complicated dynamics. We just mention the homoclinic explosion generating the Lorenz attractor, see e.g. [Sparrow] (1982), and the celebrated example

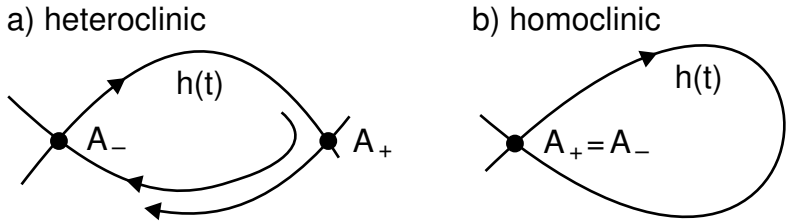

Figure 1.1: A heteroclinic orbit (a) and a homoclinic orbit (b).

due to Shilnikov, generating shift dynamics for flows. See examples 2.2, 5.4, 5.8, and definition 2.3 below.

Partial differential equations are another important source of applications. We explicitly mention travelling waves, solitons, boundary layers in singular perturbation problems, and viscous profiles for systems of conservation laws. Already ten years ago, for example, Shilnikov type shift dynamics have been discovered for travelling waves of the FitzHugh-Nagumo model of nerve conduction, see [Evans et al.] (1982), [Feroe] (1982), [Hastings] (1982).

An embracing systematic theory of homoclinic bifurcations in two parameter systems, $\lambda \in \mathbb{R}^2$, is not in sight. Rather, there appear to be hundreds of different cases which need to be analyzed separately. Some of the cases which have been analyzed successfully, so far, will be discussed in the present paper. In fact we will not add to that list. Instead we will introduce some new concepts, based on a few relevant examples, which allow for a global *pathfollowing approach* to homoclinic bifurcation. Essentially we try to follow paths of homoclinic orbits up to regions in parameter and phase space with complicated recurrent dynamics. Our main result in this direction, theorem 3.4, is formulated in terms of the new concepts: *tame* versus *chaotic* homoclinic orbits, *stratified* codimension 2 *loops*, and ϵ-*length*. The concept of stratification is open in the following sense: given a particular codimension 2 homoclinic or heteroclinic loop, it may not at all be obvious, whether this loop is stratified or not. We discuss some examples below, where this question has been settled. In general, the question is open. Our theorem, as it is formulated here, can only improve in the future, when more and more particular cases of homoclinic bifurcation will be understood.

We conclude this section with an outline of the paper. The new concepts mentioned above are introduced in section 2, together with a select few examples. Section 3 explains our global continuation idea, in those terms, and

presents the main result, theorem 3.4. Proofs are relegated to section 4. In section 5, we demonstrate how our continuation process works for some, mostly local, examples from the literature. Two more globally-minded examples are designed, with an inclination towards chaos, in section 6. We finish with a detailed discussion of scope, significance, and limitations of our results, in section 7.

Acknowledgement.

Many colleagues have contributed to this paper with helpful advice and generously shared insight. In particular I would like to mention Velja Afraimovich, Jay Alexander, Don Aronson, Shui-Nee Chow, Gerhard Dangelmayr, Bo Deng, Kazimierz Gęba, Jörg Härterich, Ale Jan Homburg, Klaus Kirchgässner, John Mallet-Paret, Alexander Mielke, Björn Sandstede, Arnd Scheel, Floris Takens, André Vanderbauwhede, and J. Yorke. For careful, efficient and reliable typesetting I am much indebted to E. Schlumberger.

This work was partially supported by the Deutsche Forschungsgemeinschaft, the European Stimulation Program "Bifurcation Theory", the Landesschwerpunkt "Nichtlineare Dynamik kontinuierlicher Systeme" Baden-Württemberg, a fellowship at Konrad-Zuse-Zentrum Berlin, and by the Institut für Angewandte Analysis und Stochastik Berlin.

2 Basic examples and definitions

In this section, we collect and organize some known results and examples related to homoclinic bifurcation. Based on five examples, we introduce the notions of *tame* versus *chaotic* homoclinic orbits, of *ϵ-length*, and of *stratified* homoclinic or heteroclinic loops. These concepts are central to our subsequent analysis.

2.1 Example: B-point

Consider the planar, two-parameter system

$$\begin{aligned} \dot{x}_1 &= x_2 \\ \dot{x}_2 &= \lambda_1 + \lambda_2 x_1 + x_1^2 + x_1 x_2. \end{aligned} \tag{2.1}$$

As noticed by [Arnol'd] (1972), [Takens] (1974), system (2.1) describes the generic local normal form of an equilibrium with algebraically double eigenvalue zero, truncated at second order, and unfolded on the linear level.

In parameter space $\lambda = (\lambda_1, \lambda_2) \in \Lambda = \mathbb{R}^2$, the bifurcation diagram of figure 2.1 has been obtained by [Bogdanov] (1976). See also the accounts in [Arnol'd] (1983) and [Guckenheimer & Holmes] (1990). Crossing the fold curve in figure 2.1 from right to left, two equilibria appear by saddle-node bifurcation. Crossing the Hopf line, one of these equilibria undergoes a Hopf bifurcation. Crossing the hom line, the generated periodic orbit becomes homoclinic to the associated saddle equilibrium, and disappears. Moving the parameter λ along the hom curve towards the B-point at $\lambda = (0,0)$, the homoclinic orbits shrink to the equilibrium $x = 0$ in phase space.

System (2.1) is universal, as was proved by [Bogdanov] (1976). In fact, consider a general smooth two-parameter system

$$\dot{x} = f(\lambda, x), \quad \lambda \in \Lambda = \mathbb{R}^2, \qquad x \in X = \mathbb{R}^N, \tag{2.2}$$

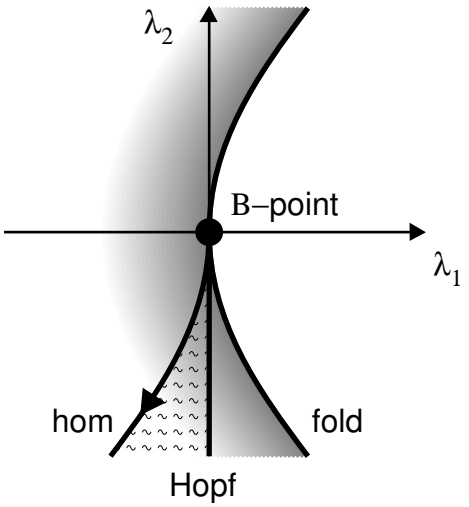

Figure 2.1: Bifurcation diagram of a B-point, example 2.1.

with an equilibrium at $(\lambda_0, x_0) = (0, 0)$. Assume the linearization $D_x f(\lambda_0, x_0)$ possesses, aside from a hyperbolic part, an algebraically double eigenvalue zero with precisely one 2×2 Jordan block. Then, locally in a center manifold, system (2.2) can be transformed to form (2.1), provided a certain nondegeneracy condition holds. The transformation is diffeomorphic in λ, homeomorphic in x, and possibly requires a reversal of time. In particular, the bifurcation diagram of figure 2.1 still holds locally.

For brevity, we call the Arnol'd-Bogdanov-Takens singularity (λ_0, x_0) a *B-point* henceforth. More precisely, we require in addition to the above nondegeneracy assumptions that the B-point itself is not associated to any (large) homoclinic orbit. We note here that these assumptions are all generic in the sense of definition 2.4 below.

B-points play a central role for global bifurcation of periodic orbits in systems with one or two parameters [Fiedler] (1986 b). It is our main goal, in

this paper, to show how B-points play an equally important role for global pathfollowing of homoclinic orbits in two-parameter flows. Intuitively, B-points serve as a source of homoclinic branches, in two parameters, in very much the same way as Hopf bifurcations, in one parameter families, serve as a source of branches of periodic orbits.

The similarity between periodic and homoclinic bifurcations will in fact be more than a superficial analogy. Viewing homoclinic orbits as limits of nearby periodic orbits will serve as our basic technical tool for global continuation. Therefore we now consider some examples of homoclinic orbits which generate unique, nearby hyperbolic periodic orbits or shift dynamics, respectively.

2.2 Example: one-parameter homoclinics

Consider a smooth one-parameter family

(2.3) $\qquad \dot{x} = f(\lambda, x),$

$\lambda \in \mathbb{R}$, $x \in X = \mathbb{R}^N$, with a homoclinic orbit $x = h(t)$ and associated equilibrium $x = A_0$ at $\lambda = \lambda_0 = 0$. Let spec denote the spectrum of the linearization $D_x f(\lambda_0, A_0)$. The principal eigenvalues $\mu_\pm$ are those elements of spec with $\pm Re \geq 0$ closest to the imaginary axis. We assume $\mu_\pm$ to be simple and, up to complex conjugacy, unique. We distinguish five cases:

(2.4.a) spec is hyperbolic, and the principal eigenvalues $\mu_\pm$ are both real with $\mu_+ + \mu_- \neq 0$;

(2.4.b) spec is hyperbolic, and $\{\mu_+, \overline{\mu}_+\}$, $\{\mu_-, \overline{\mu}_-\}$ are each conjugate complex pairs with $Re\mu_+ + Re\mu_- \neq 0$;

(2.5.a) spec is hyperbolic, and one of $\mu_\pm$ is real while the other forms a complex conjugate pair such that the real part of the complex

pair is *larger* than the real eigenvalue, in absolute value;

(2.5.b) spec is as in (2.5.a), but the real part of the complex pair is *less* than the real eigenvalue, in absolute value;

(2.6) $\mu_+ = \mu_- = 0$ is just one simple eigenvalue, and (λ_0, A_0) lies on a nondegenerate quadratic, stationary fold $\lambda = \lambda(\sigma),\ A = A(\sigma)$ such that $A(0) = A_0,\ A'(0) \neq 0;\ \lambda(0) = \lambda_0,\ \lambda'(0) = 0,\ \lambda''(0) \neq 0.$

In the hyperbolic cases (2.4) and (2.5), the equilibria near A_0 are parametrized over λ as $A = A(\lambda)$ locally near $\lambda = \lambda_0$, by the implicit function theorem. We obtain associated unstable and stable manifolds $W^u = \bigcup_\lambda W^u_\lambda$, $W^s = \bigcup_\lambda W^s_\lambda$, which we may consider as immersed submanifolds of $\mathbb{R} \times X$, fibered over the parameter $\lambda \in \mathbb{R}$, by smooth dependence on parameters. We assume

(2.7) $W^u \pitchfork W^s$ along (λ_0, h) in $\mathbb{R} \times X$.

As usual, $\pitchfork$ indicates transverse intersection: at any intersection point the two tangent spaces together span the whole space $\mathbb{R} \times X$. Watching the fibers W^u_λ, W^s_λ, we can express this assumption by saying that W^u_λ, W^s_λ cross each other, along h, at $\lambda = \lambda_0$ with nonzero speed.

In the fold case, by assumption (2.6), the stable set

$$W^s_{\lambda_0}(A_0) := \{x_0 \mid x(t) \to A_0 \text{ for } t \to +\infty\}$$

is also an immersed submanifold of $X = \mathbb{R}^N$ with boundary given by the strong stable manifold $W^{ss}_{\lambda_0}(A_0)$. Similarly, $W^u_{\lambda_0}(A_0)$, the unstable set, will be an immersed submanifold with boundary $W^{uu}_{\lambda_0}(A_0)$. We assume transversality again:

(2.8) $W^s_{\lambda_0}(A_0) \pitchfork W^u_{\lambda_0}(A_0)$ along h in X.

Note that we have fixed the λ_0-fiber, this time, requiring that the tangent

spaces of the *fibers* together span X. Finally we assume that

(2.9) the homoclinic orbit $h(t)$ approaches A_0 along the principal directions, that is, along the eigenspaces of $\mu_\pm$, for $t \to \mp\infty$.

Under the conditions (2.7) – (2.9), the celebrated work of [Shilnikov] (1962–1970) essentially leads to the following results. Fix a small neighborhood $\mathcal{N}$ of h in $X = \mathbb{R}^N$. In cases (2.4.a), (2.5.a), (2.6), the neighborhood $\mathcal{N}$ contains at most one non-stationary periodic orbit, for λ near λ_0. In fact, one periodic orbit exists precisely for λ on one side of $\lambda_0 \in \mathbb{R}$. The periodic orbit is hyperbolic.

In contrast, consider cases (2.4.b), (2.5.b). In these cases, $\mathcal{N}$ contains Smale horseshoes. In particular, a shift on finitely many symbols can be embedded into the given flow at, and near, $\lambda = \lambda_0$.

We condense these results into the following definition.

2.3 Definition: tame, chaotic

Consider a homoclinic orbit h as in example 2.2. In particular, assume that nondegeneracy assumptions (2.7) – (2.9) hold. We call h *tame* in cases (2.4.a), (2.5.a), (2.6). We call h *chaotic* in cases (2.4.b), (2.5.b).

In short, tame homoclinic orbits are accompanied by a unique branch of hyperbolic periodic orbits, while chaotic homoclinic orbits are accompanied by shift dynamics. The hyperbolic cases are listed in table 2.1. Note that our definition of tame and chaotic is invariant under time reversal.

We emphasize the local character of our definition of tame versus chaotic with an example due to [Shilnikov] (1969). Consider the fold case (2.6) of example 2.2 again. Conceivably, the stable and unstable sets $W^s_{\lambda_0}(A_0)$ and $W^u_{\lambda_0}(A_0)$ could intersect, transversely as in (2.8), along several distinct

eigenvalues	μ_+ real	μ_+ complex
μ_- real	tame	tame
μ_- complex	chaotic	chaotic

Table 2.1: Homoclinic orbits with principal eigenvalues $Re\mu_+ > |Re\mu_-| > 0$.

homoclinic orbits $h_1, \ldots, h_m$ simultaneously. In that case, the shift on m symbols embeds into the flow for those values of λ near λ_0, for which the equilibria have disappeared. Nevertheless, we would call each individual orbit h_j tame, because the shift dynamics is encoded by excursions along the respective orbits $h_1, \ldots, h_m$, and thus leaves a fixed small neighborhood $\mathcal{N}_j$ of h_j, in general.

The nondegeneracy assumptions entering into examples 2.1, 2.2 and definition 2.3 are somewhat awkward to explicate. To handle nondegeneracy conditions more summarily, we use the notion of genericity.

2.4 Definition: generic

Let $\mathcal{G}$ be a subset of a topological Baire space $\mathcal{F}$. We call $\mathcal{G}$ *generic* if $\mathcal{G}$ contains a countable intersection of open, dense subsets of $\mathcal{F}$. In particular, generic sets are still dense. We likewise call elements of $\mathcal{G}$ generic, as well as the properties defining $\mathcal{G}$.

In our setting, $\mathcal{F} = C^k(\Lambda \times X, X)$, $\dim \Lambda < k \leq \infty$, with the (weak) Whitney topology. For example, we claim that the zero set of $f \in \mathcal{F}$ is an embedded submanifold of $\Lambda \times X$ of dimension $\dim \Lambda$, generically. Indeed, the set $\mathcal{G}$ of such f contains the set $\mathcal{G}_0$ of f for which zero is a regular value. Clearly $\mathcal{G}_0$

is open, if $\Lambda \times X$ is any closed ball in $\mathbb{R}^2 \times \mathbb{R}^N$. By Sard's theorem, $\mathcal{G}_0$ is also dense. This proves our claim. Note that $\mathcal{F}$ is a Baire space and therefore generic subsets are always dense, see e.g. [Hirsch] (1976). A property defining $\mathcal{G}$ is said to be generic in one parameter, if $\mathcal{G}$ is generic for $\Lambda = \mathbb{R}$. Similarly, $\Lambda = \mathbb{R}^2$ defines two-parameter genericity.

2.5 Proposition

Generically, for smooth one-parameter families, homoclinic orbits are either tame or chaotic.

Proof:

The proof proceeds very much along the lines of the Kupka-Smale theorem, see for example [Abraham & Robbin] (1967). For a list of generic one parameter bifurcations of stationary and periodic solutions see [Fiedler, proposition 1.1] (1986 b). Genericity of the transversality assumptions (2.7), (2.8) follows as for the Kupka-Smale theorem. Note, however, that

$$\dot{h} \in T_h W^s \cap T_h W^u$$

requires the additional parameter $\lambda \in \mathbb{R}$ in order that transversality holds. Once we restrict the parameter value $\lambda = \lambda_0$ to belong to a homoclinic orbit h we may perturb the eigenvalue structure at the equilibrium, such that indeed one of the cases (2.4) - (2.6) occurs for the principal eigenvalues. Assumption (2.9) is generic, by small perturbations along the homoclinic orbit h. This completes a sketch of proof of proposition 2.5. For more detailed genericity arguments, we also refer to [Fiedler] (1985). □

We now return to two parameters $\lambda = (\lambda_1, \lambda_2) \in \Lambda = \mathbb{R}^2$. We will restrict our attention to generic phenomena. Generically, equilibria are then

(2.10) (i) hyperbolic, or

(ii) nondegenerate folds, or

(iii) Hopf points, or

(iv) cusps, or

(v) fold-Hopf points, or

(vi) B-points, or

(vii) Hopf-Hopf points.

See e.g. [Fiedler, proposition 1.4] (1986 b) and the references there, as well as [Arnol'd] (1972), [Guckenheimer & Holmes] (1990). Case (i) occurs for open regions in parameter space Λ, cases (ii), (iii) along differentiable curves. Cases (iv) – (vii) occur at isolated parameter values, if the set of equilibria is bounded in X. We will return to some of these cases later. Unfortunately, case (vii) was omitted in [Fiedler] (1986 b); it describes equilibria with two distinct non-resonant pairs of purely imaginary eigenvalues, all simple. Fortunately, this case does not affect any of the results proved there.

As we have seen for the B-point, example 2.1, homoclinic orbits occur along curves in two-parameter problems. In particular, a tame homoclinic orbit in a one-parameter problem gives rise to a local path γ of tame homoclinic orbits, in two parameters. Our notion of tame then refers to restricting λ to one-dimensional curves which intersect the homoclinic path transversely. This way, we may talk about *tame paths*.

Taking a more global point of view, we ask for limits of homoclinic orbits, for example along a tame path. This question leads to our definition of the ϵ-length of a homoclinic orbit.

2.6 Definition: ϵ-length

Fix $\epsilon > 0$. Let $\mathcal{E} = \mathcal{E}(\lambda) \subseteq X$ denote the set of equilibria and $U_\epsilon(\mathcal{E})$ its open ϵ-neighborhood. Let h denote a homoclinic orbit of $f(\lambda, \cdot)$. We call

$$\ell_\epsilon(h) := \text{length of } h \text{ outside } U_\epsilon(\mathcal{E})$$

the *ϵ-length* of h. Note that

$$\ell(h) := \lim_{\epsilon \downarrow 0} \ell_\epsilon(h) = \int_{-\infty}^{+\infty} |\dot{h}(t)|_2 \mathrm{d}t \leq \infty$$

is the length of the homoclinic orbit h. Similarly, we can define the ϵ-length of any, not necessarily homoclinic orbit.

We say that a set (or a path) of orbits has *unbounded ϵ-length*, if $\ell_\epsilon(\cdot)$ is unbounded on this set for some, and hence for all, small ϵ. In contrast, we say that the set has *bounded ϵ-length*, if $\ell_\epsilon(\cdot)$ is bounded for each $\epsilon > 0$, but not necessarily uniformly in ϵ.

2.7 Example: fold-Hopf

In principle, a set of homoclinic orbits with bounded ϵ-length $\ell_\epsilon(\cdot)$ can have length $\ell(\cdot)$ unbounded.

Fold-Hopf points in $X = \mathbb{R}^3$ with eigenvalues $0, \pm i$ provide specific examples. Unlike B-points, a universal unfolding has not been established for the fold-Hopf (and probably does not exist). We recall some results for the truncated normal form here. See [Guckenheimer & Holmes, §7.4] (1990) for more details on the local analysis. In cylindrical coordinates coordinates (r, φ, z) for $x \in \mathbb{R}^3$, the linearly unfolded truncated normal form reads

$$\begin{aligned} \dot{r} &= \lambda_1 r + \alpha r z, \\ \dot{z} &= \lambda_2 + \beta r^2 - z^2, \end{aligned} \tag{2.11}$$

with fixed parameters $\alpha \in \mathbb{R}$ and $\beta = \pm 1$. Note that the angle coordinate

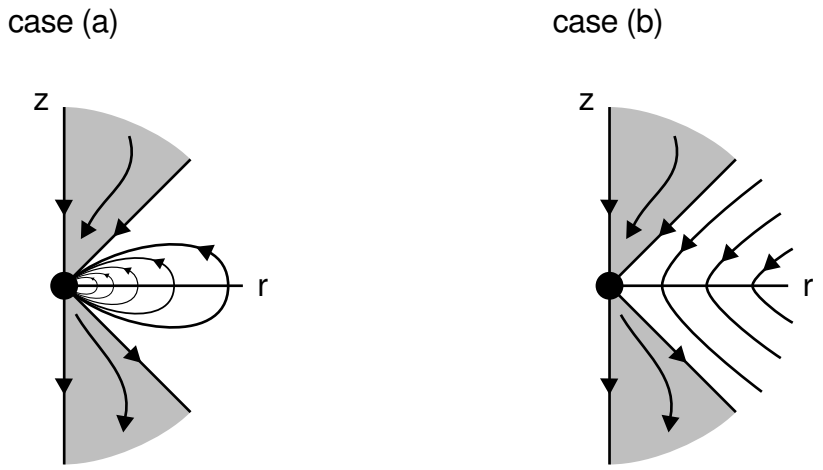

Figure 2.2: Local phase portraits of (2.11) for cases (a), (b), $\lambda = 0$.

φ associated to the radius r does not appear because of S^1-equivariance of the normal form. Moreover $|\dot{\varphi}| \approx 1$ is uniformly bounded below. We only mention two particular cases of several inequivalent bifurcation diagrams here:

(a) $-1 < \alpha < 0, \beta = +1$, and
(b) $\alpha < -1, \beta = -1$.

Local phase portraits, at $\lambda = 0, r = z = 0$, obtained by a blow-up technique, are given in figures 2.2.a,b. Note the shaded sectors, solid cones in $\mathbb{R}^3$. In either case, these sectors allow for two-parameter families of large homoclinic orbits towards $x = 0$ in $\mathbb{R}^3$, with λ fixed at $\lambda = 0$.

In case (b), the boundaries of the shaded sector could belong to the same trajectory, globally. Breaking the S^1-equivariance of the normal form, by higher order or flat terms, the two-dimensional boundaries in $\mathbb{R}^3$ can be assumed to intersect transversely. This would imply recurrent behavior of shift type, even at $\lambda = 0$.

Consider case (a) next. Analyzing the local unfolding, as in [Guckenheimer

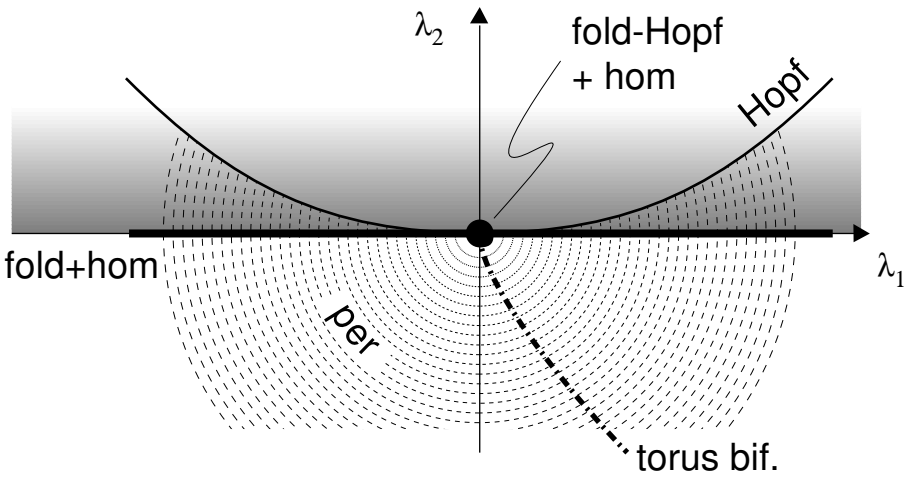

Figure 2.3: A possible bifurcation diagram for case (a).

& Holmes] (1990), large homoclinic orbits cannot exist for $\lambda_2 \neq 0$. Indeed, there are no equilibria for $\lambda_2 < 0$. For $\lambda_2 \geq \lambda_1^2/\alpha^2$, one of the two equilibria is a local attractor while the other is a repeller. For $0 < \lambda_2 < \lambda_1^2/\alpha^2$, the only saddle equilibrium connects to a unique periodic orbit. In either region, homoclinic orbits cannot occur. Note, however, the possibility of a persistent large homoclinic orbit along the fold curve $\lambda_2 = 0$. See figure 2.3.

Following such a hom branch, which locally coincides with the fold branch in Λ, the homoclinic orbits typically develop unbounded length while their ϵ-length remains bounded. Indeed, for $|\lambda_1|$ small, consider the intersection points $h_\pm = h_\pm(\lambda_1)$ of the homoclinic orbit h with a fixed small neighborhood of the fold-Hopf point. From that (large positive or negative) time t on, the normal form (2.11) describes $h(t)$ well. Passing to the fold-Hopf limit $\lambda_1 = 0$, we may assume that $h_\pm(\lambda_1 = 0)$ does not lie on the z-axis, generically. By blow-up arguments, the quotient

$$\lim_{t \to \pm\infty} z(t)/r(t) = q_\pm$$

then exists and is finite, at $\lambda_1 = 0$; see figure 2.2(a). In particular, (2.11)

implies

$$|\dot{r}(t)| \leq c_2 r(t)^2$$

for some $c_2 > |\alpha q_\pm|$ and for $|t|$ large enough. Therefore

$$r(t) \geq c_3/|t|,$$

for some $c_3 > 0$ and all $|t|$ large. On the other hand, since $|\dot{\varphi}| \approx 1$ is bounded below,

$$\int |\dot{h}(t)| \mathrm{d}t \geq \int r(t) |\dot{\varphi}(t)| \mathrm{d}t \geq c_1 \int r(t) \mathrm{d}t, \tag{2.12}$$

for some positive c_1. By our lower estimate on $r(t)$ the integral (2.12) diverges and the length of h becomes unbounded for $\lambda_1 \searrow 0$. Clearly the ϵ-length of h will remain bounded, e.g., if the time h spends outside our fixed neighborhood of the fold-Hopf point is uniformly bounded. We return to this example in section 5.5.

Tame homoclinic orbits, by transversality, can be continued locally to form a tame path as we have seen above. We now consider limits of homoclinic orbits of bounded ϵ-length.

Consider a bounded sequence of homoclinic or heteroclinic orbits $h_n(\cdot)$ of uniformly locally Lipschitz vector fields

$$\dot{x} = f_n(x) \tag{2.13}$$

in X. In other words, the α- and ω-limit sets $\alpha(h_n), \omega(h_n)$ are contained in the respective sets $\mathcal{E}_n$ of equilibria of f_n. Assume

$$f = \lim_{n \to \infty} f_n \tag{2.14}$$

exists, locally uniformly. Let

$$H := \{x \in X \mid x = \lim_{m \to \infty} x_m \text{ holds for some sequences } x_m \in h_{n_m}, n_m \nearrow \infty\} \tag{2.15}$$

be the set of limiting points of the sequence $h_n(\cdot)$.

2.8 Proposition: loops

In the above setting, assume the sequence $h_n(\cdot)$ and the ϵ-lengths of the sequence $h_n(\cdot)$ are bounded, uniformly in n and for each fixed $\epsilon > 0$. Then H is nonempty, compact, and consists of equilibria, of homoclinic, and of heteroclinic orbits only.

In addition, assume that there exists a converging sequence $A_n \in clos(h_n)$. Then H is also connected. We call such a set H a *loop*.

Proof.

We will show that

(2.16) $\qquad \omega(x_0) \subseteq \mathcal{E},$

for all $x_0 \in H \setminus \mathcal{E}$. Here $\mathcal{E}$ denotes the set of equilibria of f. Reversing time, $\alpha(x_0) \subseteq \mathcal{E}$ follows analogously. Therefore, all non-stationary orbits in H are then homoclinic or heteroclinic, as claimed. Clearly, the ϵ-length of H is bounded by $\sup \ell_\epsilon(h_n)$. (Note that we do not require convergence to a single equilibrium $A_\pm$ here, thus extending our original definitions slightly. Generically the set $\mathcal{E}$ is discrete by our list (2.10), and therefore $\omega(x_0)$, $\alpha(x_0)$ will be single points.)

To show (2.16), we proceed indirectly. Suppose there exists $\xi \in \omega(x_0) \setminus \mathcal{E}$. Let $x(\cdot)$ denote the solution of $\dot{x} = f(x)$ with $x(0) = x_0$. Suppose $x(\cdot)$ is not periodic. Then existence of ξ implies

(2.17) $\qquad \ell_\epsilon(x(\cdot)) = \infty$, for all $\epsilon < dist(\xi, \mathcal{E})$.

Indeed, note that $x(\cdot)$ must reenter a flow box around ξ infinitely often, at distinct points. Now consider a convergent (sub-)sequence

(2.18) $\qquad x_m = h_m(0) \underset{m\to\infty}{\longrightarrow} x_0 \in H,$

according to (2.15). By continuous dependence on initial conditions, (2.17)

implies

(2.19) $\qquad \ell_\epsilon(h_m(\cdot)) \underset{m\to\infty}{\longrightarrow} \infty$

is unbounded, contrary to our boundedness assumption on $\ell_\epsilon(h_m(\cdot))$. This contradiction completes the proof for non-periodic $x(\cdot)$.

If $x(\cdot)$ is periodic, still the $h_m(\cdot)$ cannot be periodic because they were assumed to be homoclinic or heteroclinic. Therefore, (2.18) still implies (2.19).

Compactness and connectedness of H follow from [Whyburn] (1968) as in [Fiedler, lemma 7.1] (1988). This completes the proof. □

It is worthwhile to reinterpret the proposition in terms of generic two parameter vector fields for which $f_n = f(\lambda_n, \cdot)$, $\lambda_n \to \lambda$. The set $\mathcal{E}$ of equilibria of $f(\lambda, \cdot)$ is then discrete by genericity, recalling our list (2.10). In principle, the limiting loop H can contain infinitely many homoclinic or heteroclinic orbits. In our generic setting, however, this is clearly impossible by the local flow structure near equilibrium, except perhaps at a fold-Hopf point, cf. figure 2.2.a. Even in that case, however, at most finitely many orbits of H will leave a fixed ϵ-neighborhood of $\mathcal{E}$, the remaining ones being locally homoclinic to the fold-Hopf point.

We consider two specific generic examples, next, where tame paths of homoclinic orbits limit onto more degenerate codimension two homoclinic orbits.

2.9 Example: resonant homoclinic

One way to produce degenerate, codimension two homoclinic bifurcations is by violating nondegeneracy conditions of our generic one-parameter examples 2.2. Here we violate the nonresonance condition (2.4.a), $\mu_+ + \mu_- \neq 0$, for the real principal eigenvalues $\mu_\pm$ of the hyperbolic equilibrium A_0 associated

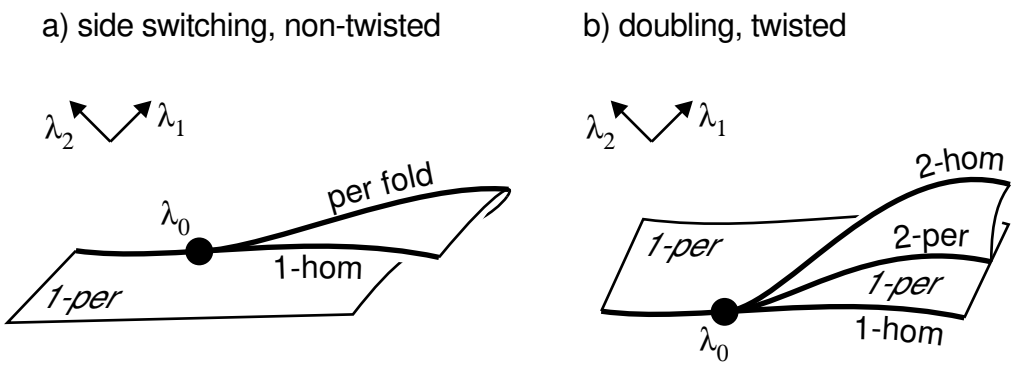

Figure 2.4: Resonant homoclinic bifurcations.

to the homoclinic orbit. Let us assume

(2.20) $\qquad \mu_+ + \mu_- = 0,$

at some parameter $\lambda = \lambda_0 \in \Lambda = \mathbb{R}^2$. Under additional nondegeneracy assumptions which are generic in two-parameter vector fields, this situation was analyzed in detail in [Chow et al.] (1990 a). Depending on a global twist condition, one of the two alternatives described in figures 2.4(a,b) is selected. In both cases there is a local path of 1-hom(oclinic) orbits, tame except for the bifurcation point $\lambda = \lambda_0$. In analogy to period doubling, we distinguish here between 1-hom and 2-hom orbits near bifurcation: where 1-hom orbits traverse a fixed small Poincaré section to the flow only once, 2-hom orbits do so twice. In case b), there is a tame branch of 2-hom orbits limiting, as a set, onto the 1-hom orbit at $\lambda = \lambda_0$. Note that the corresponding ϵ-lengths limit onto twice the ϵ-length of the limiting 1-hom orbit, for any small $\epsilon > 0$.

All tame hom paths are accompanied by per(iodic) sheets. In case a), the per sheet develops a fold and limits onto the hom path from opposite sides, on opposite sides of the bifurcation point. Hence the name *resonant homoclinic side switching*.

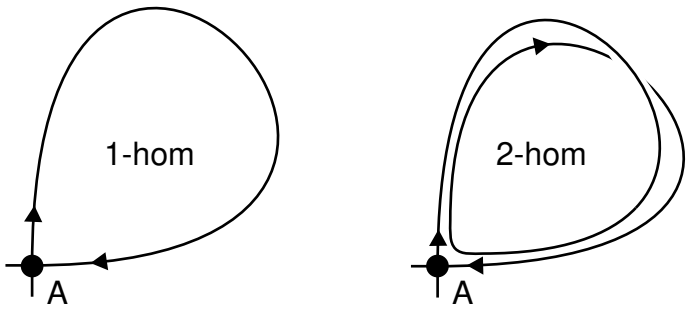

Figure 2.5: Phase portraits of 1-hom and 2-hom orbits.

In case b), the 1-per sheet limits onto the 1-hom path from just one side. The bifurcating 2-hom path generates a 2-per sheet which limits onto the 1-per sheet, at its other boundary, along a path of periodic orbits with Floquet multiplier -1: classical period doubling. We have termed this case *resonant homoclinic doubling*. Notably the bifurcations in both cases are exponentially flat, not of any algebraic order.

Resonant homoclinic side switching was discovered, in the plane, by [Leontovich] (1951). Resonant homoclinic doubling, in contrast, occurs in its simplest form at eigenvalue resonance in a Möbius strip. This properly accounts for the global twist condition mentioned above. For a first investigation of several non-chaotic homoclinic doubling mechanisms in $\mathbb{R}^3$ see [Yanagida] (1987). Notably, [Kisaka et al.] (1992) prove, in the general generic case considered here, that no further homoclinic orbits bifurcate: there are no bifurcating n-hom orbits with $n \geq 2$ (case a)), $n \geq 3$ (case b)), respectively. By [Sandstede] (1992), the same statement also holds for n-per orbits. More precisely, if a sequence of n_k-hom or n_k-per orbits $(\lambda_k, x_k(\cdot))$ limits onto the resonant homoclinic orbit, $n \geq 2$ or $n \geq 3$ respectively, then $n_k \to \infty$ as $k \to \infty$. Moreover, the 2-per sheet in case b) is confined in between the per doubling and the 2-hom path in parameter space Λ.

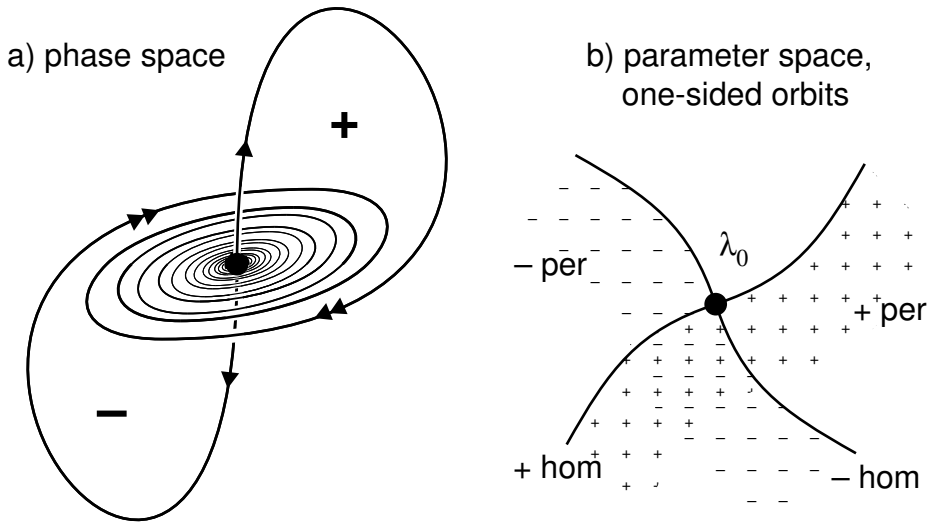

Figure 2.6: Tresser's tame 8.

2.10 Example: Tresser's tame 8, saddle focus

Tame homoclinic paths may cross each other, in two parameters and associated to the same equilibrium, see figures 2.6, 2.7. Such a crossing can produce very intricate bifurcation patterns; [Tresser] (1984) has provided a very interesting example analyzed in more detail by [Gambaudo] (1987). At the transverse intersection point $\lambda = \lambda_0$ of the tame paths, it is assumed that (2.5.a) holds for the principal eigenvalues $\mu_\pm$; specifically suppose

(2.21) $\qquad 0 < \mu_+ < -Re\mu_-.$

Moreover, let the unstable dimension be one. We assume the geometric situation of figure 2.6, that is,

$$\dot{x}(t)/|\dot{x}(t)|$$

limits onto opposite eigendirections of μ_+ along the two homoclinic orbits, for $t \to -\infty$. By these assumptions, the "figure 8" formed by the two homoclinic orbits is an attractor. As in the previous example, the two-

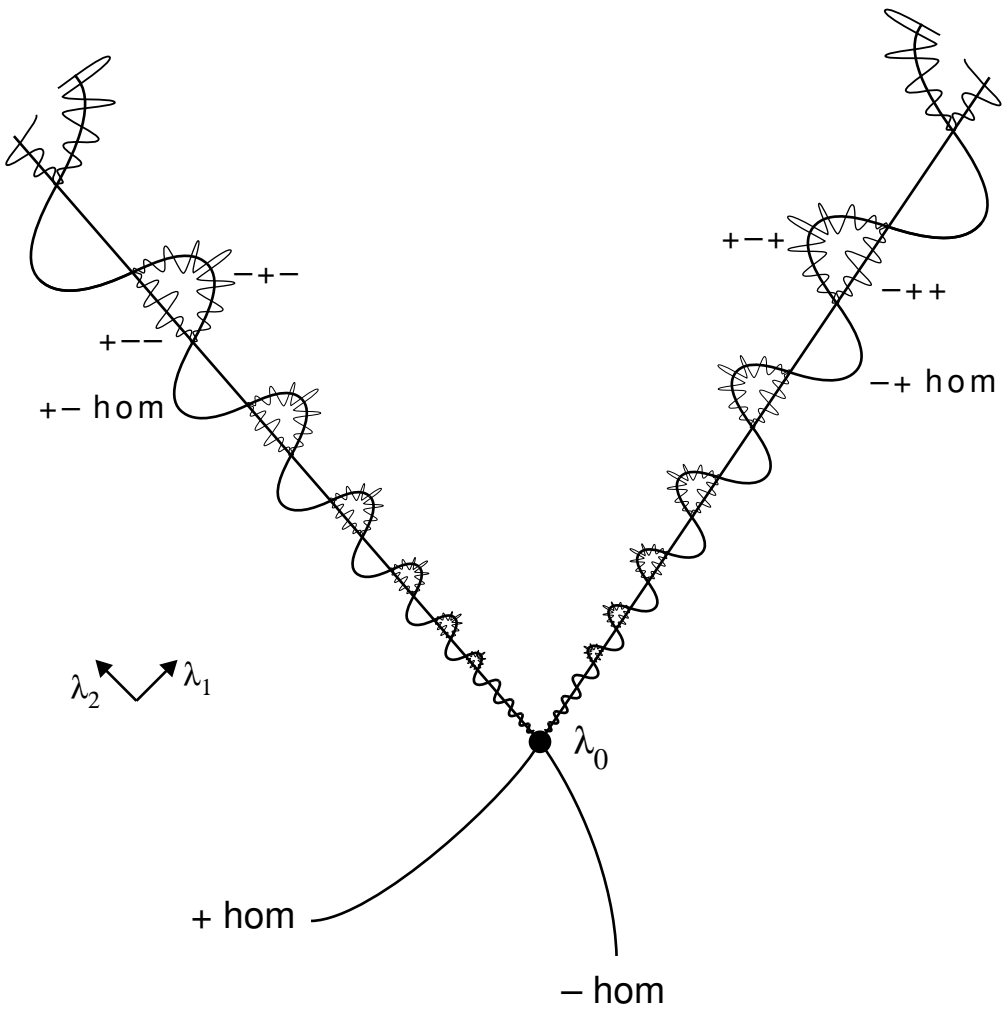

Figure 2.7: Two-parameter bifurcation diagram for Tresser's tame 8.

parameter bifurcation diagram depends on a certain global twist quantity along the homoclinic orbits. Here, we assume both homoclinic orbits to be non-twisted.

The bifurcation diagram of only some homoclinic orbits is sketched in figure 2.7. The hom paths are labeled by finite sequences of $\pm$ signs, according to their excursions along the original $\pm$homoclinic orbits. Descriptively, there is a $-+$hom path, oscillating into $\lambda = \lambda_0$ around the $+$hom path. At any intersection point of these two paths, the original bifurcation pattern at $\lambda = \lambda_0$ is re-ignited with $-$ replaced by $-+$. By this "self-similarity" arbitrarily long (but not all) finite sequences of the symbols $+, -$ occur in the bifurcation diagram of figure 2.7, under generic assumptions. For a more complete description using Farey sequences, see [Gambaudo] (1987). Note that homoclinic orbits of all these types accumulate at the bifurcation point $\lambda = \lambda_0$. A similar accumulation occurs at all the other intersection points.

Examples 2.1, 2.2, 2.7, 2.9, 2.10 give a first impression of the complexity of homoclinic bifurcations in two-parameter space $\lambda \in \Lambda = \mathbb{R}^2$. We now distinguish a class of "simple" bifurcations, which we call *stratified*. Recall from proposition 2.8, that bounded sequences of homoclinic orbits with bounded ϵ-lengths limit onto a loop H: a compact connected set in which every trajectory tends to equilibrium for $t \to \pm\infty$. In the following we use loop in that sense; to avoid trivial cases, we also assume that a loop does not consist of just a single tame or chaotic homoclinic orbit. Excluding generic codimension one "loops", we will thus focus on codimension two phenomena.

2.11 Definition: stratified

Let $H \subseteq X$ be a loop at $\lambda = \lambda_0 \in \Lambda$. We call $\{\lambda_0\} \times H$ *stratified*, if there exist closed bounded neighborhoods V_λ of λ_0 in Λ and V_x of H in X such

that (i), (ii) below both hold.

(i) $V_\lambda \setminus \{\lambda_0\}$ contains only finitely many paths of homoclinic orbits in V_x; all these paths are tame, of bounded ϵ-length, and do not touch the boundary of V_x, but leave $V_\lambda \times V_x$ through the boundary of V_λ.

For some smooth closed Jordan curve S in $V_\lambda \setminus \{\lambda_0\}$, transverse to the tame paths, and for any continuum (i.e. locally compact, connected set) $\mathcal{C} \subseteq S \times V_x$ of periodic orbits which contains a Hopf bifurcation point or a homoclinic orbit in its closure, we also require

(ii) the periodic orbits in $\mathcal{C}$ do not touch the boundary of V_x, and any sequence of periodic orbits in $\mathcal{C}$ with unbounded *virtual periods* contains a subsequence converging to a homoclinic orbit, as a set.

Above, τ is called a virtual period of a periodic orbit $p(\cdot)$ with minimal period T if τ is the minimal period of a pair $(p(\cdot), q(\cdot))$, where $q(\cdot)$ solves the linearized equation along $p(\cdot)$. In particular $\tau = mT$, for some integer m. If $m \neq 1$, then $p(\cdot)$ possesses nontrivial Floquet multipliers which are m-th roots of unity. The notion of virtual period was introduced in [Mallet-Paret & Yorke] (1982), [Chow et al.] (1983); see also [Fiedler] (1988). Effectively, virtual periods provide a necessary criterion for bifurcation: limits of minimal periods of $p_n(\cdot)$ are virtual periods of the limit $p(\cdot)$.

Note that the B-point, example 2.1, is stratified. Also, we expect the two resonant homoclinic bifurcations of example 2.9 to be stratified; see the discussion in section 7. According to our discussion, the fold-Hopf example 2.7(a) is stratified but 2.10, Tresser's tame 8, is not. More precisely, let H_1^* indicate the homoclinic orbit $+$, whereas H_2^* indicates $-$, and H_3^* is the union

of both. Then H_1^*, H_2^* will be "stratified", separately, since they are tame. But their union, H_3^*, is not stratified.

3 Global continuation

We develop our main result in this section. In section 2 we have set up the distinction between tame and chaotic homoclinic orbits, we have introduced the concept of ϵ-length, and we have discussed stratified loops of codimension 2; see definitions 2.3, 2.6, 2.11. From now on, we consider vector fields

(3.1) $\qquad \dot{x} = f(\lambda, x)$

with two-dimensional real parameter $\lambda \in \Lambda$ and real N-dimensional $x \in X$.

In two parameters, tame homoclinic orbits typically occur along one-dimensional curves. Below, we define an orientation for such curves (definition 3.1). The orientation matches, locally near the B-points of example 2.1, an index $B = \pm 1$ at these B-points. The B-index was originally designed to describe global bifurcation of periodic orbits in two-parameter flows, see [Fiedler] (1986 b). It turns out that $B = +1$ provides a source of a tame path, oriented away from the B-point as in figure 2.1, whereas $B = -1$ provides a sink; see definition 3.2 and lemma 3.3. To procure some confidence in our set-up, we indicate the consistency of the orientation of tame paths through a codimension 2 loop: the resonant homoclinic bifurcations of example 2.9. To this point, the theory has been sketched by the author in [Chow et al., pp. 233–236] (1990 a).

Our main continuation result is codified in theorem 3.4 and its variants, remarks 3.5 (i) – (iii). For bounded, oriented tame paths with bounded ϵ-length, these results basically leave the following alternatives:

(i) connecting B-points in pairs, from sources to sinks, or

(ii) hitting non-stratified loops, or

(iii) becoming chaotic.

Theorem 3.4 will be proved in section 4.

We define an orientation of (some) tame paths of homoclinic orbits as follows. Recall that a tame path γ, in parameter space Λ, is locally accompanied by hyperbolic periodic orbits $p(\cdot)$ for λ on one side of γ. The orientation of γ will be defined via an orbit index Φ of the periodic orbits $p(\cdot)$. This index has been introduced by [Mallet-Paret & Yorke] (1982) for the purpose of global continuation of periodic orbits. It is given by

$$\Phi(p(\cdot)) := \tfrac{1}{2}((-1)^{\sigma_+} + (-1)^{\sigma_+ + \sigma_-}), \tag{3.2}$$

where σ_+, σ_-, respectively, count the real Floquet multipliers of $p(\cdot)$ in $(1, \infty)$, $(-\infty, -1)$, with their algebraic multiplicity. In other words, Φ is the average of the local Brouwer fixed point indices of the first and second iterate of the Poincaré map associated to $p(\cdot)$. In particular, Φ turns out to be homotopy invariant through generic one-parameter bifurcations of periodic orbits: saddle-node bifurcation and period doubling. Note that

$$\Phi \in \{-1, 0, +1\} \tag{3.3}$$

at any hyperbolic periodic orbit.

3.1 Definition: orientation of tame paths

Let γ be a tame path, locally accompanied by periodic orbits $(\lambda, p(\cdot))$. If $\Phi(p(\cdot)) = 0$, we do not define an orientation of γ. If $\Phi(p(\cdot)) = \pm 1$, we define an *orientation* of the tame path γ such that

λ is on the right of γ, if $\Phi = +1$;
λ is on the left of γ, if $\Phi = -1$.

In other words, the orientation of γ is the induced boundary orientation in Λ, if the parameter region of the accompanying periodic orbits is given the orientation $-\Phi$.

Note that the (local) orientation of γ is well-defined, because σ_+, σ_- do not change as long as $p(\cdot)$ remains hyperbolic. Therefore, in fact, the orientation of a path is defined consistently, as long as the path remains tame.

The orientation defined above matches the definition of a B-index given in [Fiedler] (1986 b), see definition 2.1 and lemma 2.3 there. In terms of the B-point example 2.1, figure 2.1, the B-index is defined geometrically as follows.

3.2 Definition: B-index

Let $(\lambda, x) \in \Lambda \times X$ denote a B-point. Orient the stationary fold through λ, locally in parameter space Λ, such that the parameter values of the bifurcating pair of stationary solutions are to the left of the fold. In other words, the orientation of the fold is the induced boundary orientation in Λ, if the parameter region of the bifurcating stationary solutions is given a positive orientation. Pick another point (λ', x') on the fold, near (λ, x), such that the given local orientation of the fold is from λ to λ'. Define the *B-index*

$$B(\lambda, x) := (-1)^{E(\lambda', x')}, \tag{3.4}$$

where $E(\lambda', x')$ counts the strictly positive real eigenvalues of the linearization $D_x f(\lambda', x')$ with their algebraic multiplicity.

3.3 Lemma

Any B-point generates an oriented tame path of homoclinic orbits, locally. This path is oriented

away from the B-point, if $B = +1$,

towards the B-point, if $B = -1$.

In other words, $B = +1$ indicates a source, and $B = -1$ a sink of an oriented tame path.

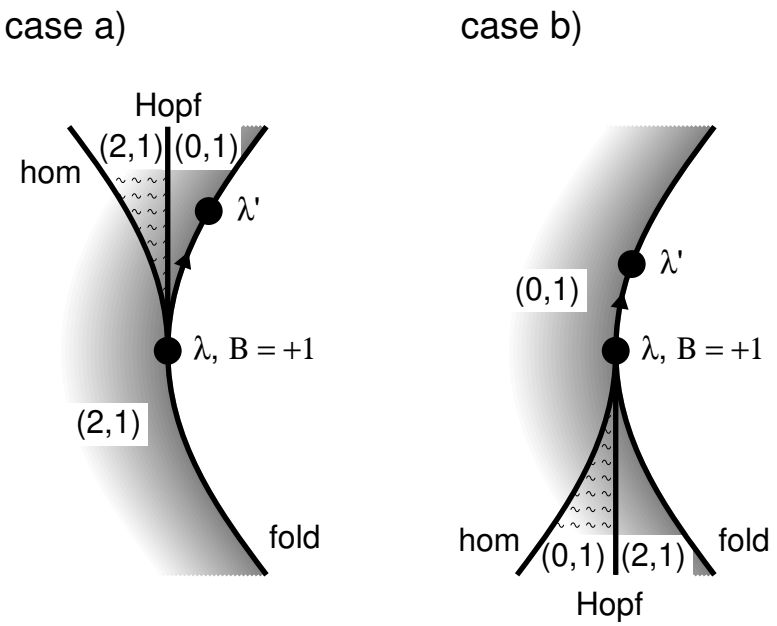

Figure 3.1: Unstable dimensions (u_1, u_2) of equilibria near B-points.

Proof.

We first show that the homoclinic path generated by a B-point (λ, x) is tame, locally. We then prove the claims about orientation. We distinguish two geometrically different bifurcation diagrams, see figure 3.1, a and b. In parameter space, the two cases are related by a reflection.

We will show below that

(3.5.a) $\Phi = B$ in case a), and

(3.5.b) $\Phi = -B$ in case b),

for the periodic orbits generated at the B-point. This will turn out to be sufficient, by our definition of an orientation of tame homoclinic paths.

Along the local homoclinic path, the associated equilibria are hyperbolic: within the two-dimensional center manifold describing the universal unfold-

ing of the B-point, as well as in full phase space X. The principal eigenvalues are real. They appear within the center manifold and describe the asymptotic decay of the homoclinic orbits. Their sum is nonzero. The tangent spaces of the stable and unstable manifold of the associated equilibria intersect one-dimensionally, along $\dot{x}$, tangent to the center manifold. Indeed, the remaining strong stable and unstable directions are inherited from the B-point. Crossing the homoclinic path in Λ transversely, the stable and unstable manifolds therefore also cross transversely, since they do so within the center manifold. Therefore, the homoclinic orbits along our path are tame, of type (2.4.a), locally near the B-point.

To prove (3.5), we may again restrict our attention to the center manifold. Indeed, a (strong) unstable dimension u, at the B-point, contributes as u to both $E(\lambda', x')$ and σ_+, in the notation of (3.2) and (3.4). This accounts for a common factor $(-1)^u$ in both

$$\Phi = \tfrac{1}{2}((-1^{\sigma_+} + (-1)^{\sigma_+ + \sigma_-}), \text{ and} \tag{3.6}$$

$$B = (-1)^{E(\lambda', x')}. \tag{3.7}$$

Note here that the Floquet exponents of the periodic orbits are, up to a small perturbation, the eigenvalues of the linearization at the B-point. In particular, σ_- is zero (or even) in (3.6) and hence can be omitted. Therefore it is sufficient to prove (3.5.a,b) or, more specifically,

$$\sigma_+ \equiv E(\lambda', x') \pmod 2, \text{ for case a}), \tag{3.8.a}$$

$$\sigma_+ \equiv E(\lambda', x') + 1 \pmod 2, \text{ for case b}), \tag{3.8.b}$$

within the center manifold of the B-point.

To prove (3.8), we may assume $E(\lambda', x') = 0$ without loss of generality. Indeed, reversing time (within the two-dimensional center manifold) changes both σ_+ and $E(\lambda', x')$ by 1. We then have to show

(3.9.a) $\sigma_+ \equiv 0 \pmod 2$, and

(3.9.b) $\sigma_+ \equiv 1 \pmod 2$,

for the respective cases.

Since $E(\lambda', x') = 0$, we can fill in the unstable dimensions of the two equilibria in the sectors of the bifurcation diagram, figure 3.1, in the form (u_1, u_2). Note that, at Hopf bifurcation, the affected equilibrium has to change its unstable dimension from 0 to 2. By elementary exchange of stability, the unstable dimensions of the equilibria at Hopf bifurcation imply

(3.10.a) $\sigma_+ = 0$,

(3.10.b) $\sigma_+ = 1$,

in the respective cases. This proves (3.9), and the lemma. □

The above proof is straightforward and, in some sense, elementary. Using the center index 中 ("zhong"), introduced in [Mallet-Paret & Yorke] (1982), and the properties of the B-index from [Fiedler] (1986 b), the proof can be recast as follows. Consider a small circle S in Λ around the B-point parameter λ. Let S be oriented positively. Then $中 = B$ at the Hopf bifurcation point on S. By exchange of stability,

(3.11.a) $\Phi = 中$,

(3.11.b) $\Phi = -中$

in cases a) and b), respectively. Again this proves (3.5), and the lemma.

In the next section we will show how the orientations of tame homoclinic paths fit together in a neighborhood V_x of a stratified codimension 2 loop at $\lambda = \lambda^*$. In fact, let η_+ denote the number of oriented paths in $\Lambda \times V_x$ with orientation towards λ^*, and let η_- count the paths directed away from λ^*. Then

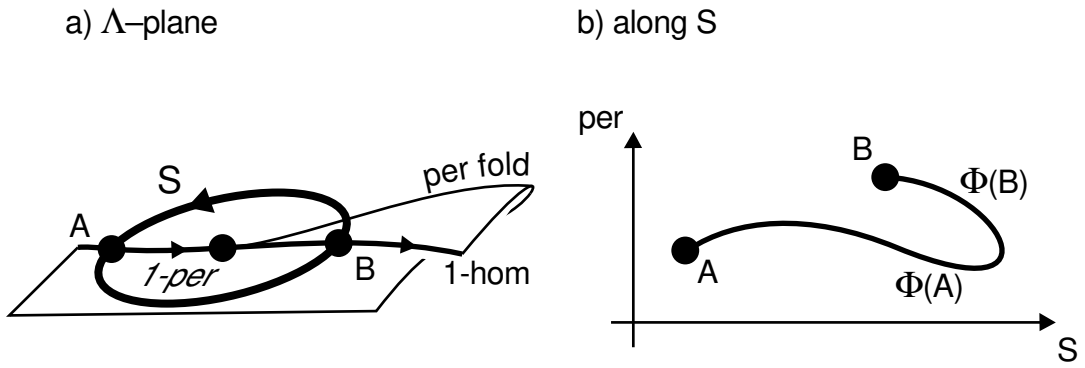

Figure 3.2: Orientations and resonant homoclinic side switching.

(3.12) $\eta_+ = \eta_-$,

as we will see in (4.4), lemma 4.1.

This crucial fact allows us to join up tame paths in pairs at any stratified loop: to any path towards the stratified loop in $\Lambda \times V_x$ we may associate, bijectively, one which leaves. In this manner, *orientations of tame paths can be extended consistently through stratified codimension 2 loops.*

We illustrate this important fact with our resonant homoclinic bifurcation examples 2.9, a) and b). Consider a), resonant homoclinic side switching, first.

For definiteness assume the geometric situation of figure 3.2.a. In figure 3.2.b, the parameters are restricted to a small, positively oriented circle S around the bifurcation point. Let $\Phi(A), \Phi(B)$ denote the periodic orbit indices near the homoclinic orbits A, B. By homotopy invariance of Φ, see [Mallet-Paret & Yorke] (1982), we obtain

(3.13) $\Phi(A) + \Phi(B) = 0.$

By definition 3.1 of orientation, this implies that either both tame half-branches are non-oriented ($\Phi(A) = 0 = \Phi(B)$), or are oriented in the same

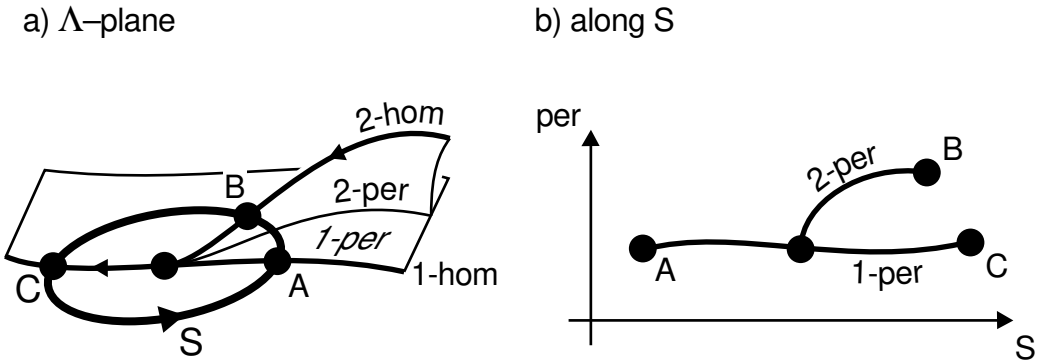

Figure 3.3: Orientations and resonant homoclinic doubling.

direction. Indeed, $0 \neq \Phi(A) = -\Phi(B)$ and the periodic orbits appear on opposite sides of the tame path, near A and B. In particular, $\eta_+ = \eta_- = +1$. The orientation in figure 3.2.a corresponds to the choice $\Phi(A) = +1$.

Consider resonant homoclinic doubling next, in the geometric situation of figure 3.3.a for definiteness. Again, figure 3.3.b shows the periodic orbits along the small, positively oriented circle S. Suppose $\Phi(C) = +1$, for example, near C. By homotopy invariance of Φ,

$$\Phi(B) + \Phi(C) = \Phi(A). \tag{3.14}$$

Since σ_- changes by 1, along the primary periodic branch at period doubling, we have

$$\sigma_-(A) \equiv \sigma_-(C) + 1 \pmod 2.$$

But $\Phi(C) \neq 0$ implies, by (3.2), that $\sigma_-(C)$ is even and we see that $\sigma_-(A)$ must be odd. In particular, $\Phi(A) = 0$, by (3.2). Therefore, (3.14) implies

$$\Phi(B) + \Phi(C) = 0, \tag{3.15}$$

similarly to the previous case. Since the periodic orbits appear on opposite sides of the tame paths, near B and C, we obtain a consistent orientation

through the bifurcation point as in figure 3.3.a. Note that $\eta_+ = \eta_- = +1$ again, as in (3.12) above. All remaining combinations of orbit indices, and all stratified homoclinic bifurcations, will be dealt with in lemma 4.1.

We are now ready to state our main result. Our formulation is in terms of smooth compact manifolds Λ, X of real dimension $2, N$, respectively. We assume Λ is oriented, so that our orientation of tame paths is defined consistently, and that X is Riemannian, so that ϵ-length is defined. All other concepts used are local, and therefore carry over to manifolds easily.

3.4 Theorem

Let Λ, X be smooth compact manifolds, X Riemannian, Λ oriented and two-dimensional. Consider smooth vector fields

$$\dot{x} = f(\lambda, x), \quad \lambda \in \Lambda, x \in X,$$

in the Whitney topology of C^k-uniform convergence, for any k. Then for generic f the following holds.

The tame homoclinic paths emanating or terminating at B-points with index $B = +1$ or $B = -1$ can be oriented. These tame oriented paths can be extended consistently through stratified codimension 2 loops until the path

(i) hits a B-point of the opposite index, or

(ii) hits a non-stratified loop, or

(iii) reaches the boundary of the set of chaotic homoclinic orbits, or

(iv) develops unbounded ϵ-length.

Here, a tame path hitting a B-point or a non-stratified loop H is understood

in the sense of proposition 2.8: the limiting set is a B-point or is contained in a non-stratified, connected loop H.

3.5 Remarks

(0) Stated loosely, we may rephrase the conclusion of the theorem as follows. Either, our oriented tame hom paths join up B-points in pairs of opposite index, (i), or else they lead into regions with complicated recurrent dynamics, (ii) – (iv).

(i) The theorem remains valid, but is weakened, if ϵ-length in (iv) is replaced by ordinary length. Indeed, unbounded ϵ-length implies unbounded length, but not conversely.

(ii) The theorem generalizes directly to the case where the total space $\Lambda \times X$ is replaced by a compact (Riemannian) fiber bundle with oriented base Λ and flow invariant fiber X. Indeed, all concepts used in the theorem and its proof are local in the parameter, although the result is global.

(iii) In applications, $\Lambda = \mathbb{R}^2$ and $X = \mathbb{R}^N$ are typically non-compact. But suppose, for example, that f is (locally uniformly) dissipative: for each λ, there exists a ball in X which attracts all bounded sets; assume this ball can be chosen uniformly for all parameters in a neighborhood of λ. Then the theorem remains valid, if we add the possibility that λ might become unbounded along the homoclinic path. In particular, the theorem then remains valid as it stands, if homoclinic orbits do not exist for large $|\lambda|$. Similarly, suppose f is not dissipative but the set of (associated) equilibria remains bounded. Then homoclinic orbits

$(\lambda, x(\cdot))$ may also become unbounded in $x(\cdot)$; but they will have to develop unbounded length along the way.

All these variants follow easily from the theorem. Just assume boundedness of the relevant homoclinic paths. Then modify f, for large λ, x, to make f dissipative and to guarantee

$$\dot{x} = f(\lambda, x) = -x, \quad \text{for } |\lambda| \text{ large.}$$

This defines a flow on the compactifications $\Lambda^c = S^2$, $X^c = S^N$, and the theorem applies.

For a more detailed discussion we refer to sections 5 – 7.

4 Proof

In this section, we prove our main result, theorem 3.4. The proof basically reduces to showing that, at a stratified loop, the same numbers of oriented tame homoclinic paths enter and leave. This step, also of independent interest, is accomplished in lemma 4.1.

We will proceed as follows. By propositions 2.5 and 2.8, homoclinic orbits arise as tame or chaotic orbits, and limit onto (stratified or non-stratified) loops, as long as ϵ-length remains bounded. To prove the theorem, we suppose that none of the cases (ii) – (iv) occurs, that is, ϵ-length stays bounded, our path stays away from the chaotic region, and only hits stratified loops. Under these assumptions we then have to show that such a path joins pairs of B-points of opposite B-index.

We clarify our notation of a path, first. Let

$$\mathcal{E}_\lambda := \{x \in X \mid f(\lambda, x) = 0\} \tag{4.1}$$

denote the set of equilibria of $f(\lambda, \cdot)$, and

$$\mathfrak{H} := \mathrm{clos}\{(\lambda, x) \in \Lambda \times X \mid x \notin \mathcal{E}_\lambda, \alpha(x) = \omega(x) \subseteq \mathcal{E}_\lambda\} \tag{4.2}$$

the closure of the set of homoclinic orbits. Note that all B-points lie in $\mathfrak{H}$, as do all loops H in the setting of proposition 2.8 with $f_n = f(\lambda_n, \cdot)$. Any maximal connected component $\mathfrak{P}$ of $\mathfrak{H}$ is called a *(global) path.*

As an interlude, consider $\mathfrak{H}$ near a B-point (λ_0, x_0). Let $\mathfrak{P}$ denote the path in $\mathfrak{H}$ containing (λ_0, x_0). For generic f, we claim that there exists a neighborhood $V \subseteq \Lambda \times X$ of (λ_0, x_0) such that $\mathfrak{P} \cap V$ consists of only the B-point and the local tame homoclinic path originating from it, provided that $\mathfrak{P}$ has bounded ϵ-length. Indeed, suppose the claim is not true. Then (λ_0, x_0) is part of a nontrivial loop H by proposition 2.8. (Note that H need not be contained in V). By genericity of the vector field $f(\lambda_0, \cdot)$ we may assume

that all equilibria in $\mathcal{E}_{\lambda_0}$ are hyperbolic, except for the B-point x_0. Moreover, the respective stable and unstable manifolds (respectively sets, for x_0) are mutually transverse. The dimensions of the stable and unstable sets of (λ_0, x_0), immersed manifolds with boundary, add up to $N = \dim X$ by local normal form analysis. Therefore, x_0 cannot be associated with a homoclinic orbit h, having $\dot{h}$ as an intersection of the tangent spaces of these sets. For the same reason, x_0 cannot belong to a circular chain of heteroclinic orbits involving other, hyperbolic equilibria. This contradiction proves our claim.

By this claim, the path emanating or terminating at a B-point is now uniquely identified, locally in Λ, as the oriented tame path from the normal form analysis of example 2.1.

Let $\mathfrak{P}$ denote a global path. Let $\mathfrak{P}'$ denote a maximal connected component of the set $\mathfrak{P}$ after all non-oriented tame paths in $\mathfrak{P}$ have been removed. Following our outline of proof, we may assume that the ϵ-length of $\mathfrak{P}'$ is bounded, $\mathfrak{P}'$ is bounded away from the chaotic region, and $\mathfrak{P}'$ contains only stratified loops. Let (λ_j, x_j) enumerate all B-points in $\mathfrak{P}'$; by compactness and genericity their number is finite. We claim

$$\sum_j B(\lambda_j, x_j) = 0. \tag{4.3}$$

To prove (4.3) we note that $\mathfrak{P}'$ has the structure of a finite oriented graph. The vertices are the B-points and the stratified loops in $\mathfrak{P}'$, and the edges are the oriented tame paths of homoclinics. Finiteness of the graph follows from bounded ϵ-length, compactness, convergence proposition 2.8, and local finiteness at each stratified vertex.

It is a somewhat subtle point here that, at the same parameter value λ^*, several loops H_j^* might belong to $\mathfrak{P}'$. For a (non-stratified) example, recall Tresser's 8 in 2.10 where again H_1^* indicates the tame homoclinic orbit $+$, H_2^* indicates $-$, and H_3^* is the non-stratified union of both. In our general

setting, we have by now required the union of the loops H_j^* at λ^* to be stratified. This allows us to ignore the individual loops H_j^*, replacing them by their union throughout.

Clearly, any B-point of $\mathfrak{P}$ is still contained in some component $\mathfrak{P}'$, by lemma 3.3. Note that a B-point (λ_j, x_j) with $B = +1$ provides a *source* of $\mathfrak{P}'$, while $B = -1$ provides a *sink*. Moreover, (4.3) follows if we prove "Kirchhoff's law" at each stratified vertex $\{\lambda^*\} \times H^*$. More precisely, let η_+ and η_- denote the number of oriented tame paths in $\mathfrak{P}'$ oriented towards (away from) λ^*, respectively, as in (3.12). As for balancing currents in an electrical network it is then equivalent to (4.3) to prove $\eta_+ = \eta_-$ at each stratified vertex $\{\lambda^*\} \times H^*$.

This fact, $\eta_+ = \eta_-$, is of independent practical significance in the analysis of homoclinic and heteroclinic bifurcations. Even in purely numerical investigations, it can provide a valuable clue to oriented tame homoclinic branches which might easily be overlooked otherwise. We single out this fact as lemma 4.1; see also figure 4.1. With the proof of this lemma, our proof of theorem 3.4 will also be complete, since the additional assumption below about absence of B-points at λ^* is generic.

4.1 Lemma

Let $\{\lambda^*\} \times H^*$ be a stratified loop with η_+ tame homoclinic paths oriented towards it and with η_- tame homoclinic paths oriented away from it. Assume that none of the equilibria associated to H^* is a B-point. Then

(4.4) $\qquad \eta_+ = \eta_- \ .$

Proof.

For the stratified loop $\{\lambda^*\} \times H^*$ we choose neighborhoods V_λ of λ^*, V_x of H^*

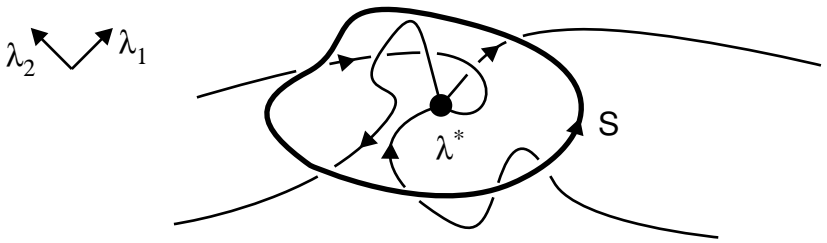

Figure 4.1: A stratified loop in parameter space.

and a smooth closed Jordan curve S in $V_\lambda \setminus \{\lambda^*\}$, as in definition 2.11. Let S be oriented positively, and restrict $f(\lambda, \cdot)$ to the one-parameter family $\lambda \in S$. By assumption, we may require that the interior of S does not contain any B-point.

The proof now consists of a careful analysis of global continua of periodic solutions along the curve S, in the spirit of [Mallet-Paret & Yorke] (1982).

First we approximate f, along S, by a sequence

(4.5) $\qquad g_n \to f$

of generic one-parameter vector fields g_n in the sense of [Mallet-Paret & Yorke] (1982), [Fiedler] (1985). Because S intersects the tame paths transversely, the tame homoclinic orbits on S persist under these small generic perturbations and remain tame.

For the generic vector fields g_n, periodic orbits are hyperbolic except at saddle-node and period doubling bifurcations along S. The orbit index

$$\Phi = \tfrac{1}{2}((-1)^{\sigma+} + (-1)^{\sigma+ + \sigma-}),$$

as defined in (3.2) has homotopy invariance properties at these bifurcations. Following [Mallet-Paret & Yorke] (1982), we may orient paths of hyperbolic periodic orbits

along S, if $\Phi = +1$,

opposite to S, if $\Phi = -1$.

If $\Phi = 0$, we do not define an orientation. Note that hyperbolic periodic orbits are parametrized over S, locally. Homotopy invariance of Φ implies that the orientation extends, consistently, through saddle-node and period doubling bifurcations. At period doubling, note that precisely two of the three half-branches are oriented: the secondary, period doubled branch and one half of the primary branch. See also the resonant homoclinic doubling example 2.9.b, figure 3.3, and (3.14), (3.15). Maximal connected sets of oriented periodic orbit paths are called *snakes*.

In [Mallet-Paret & Yorke] (1982), creation of snakes at Hopf bifurcation points (alias "centers") was also considered. Their center index Φ, mentioned above when proving lemma 3.3, is defined such that the originating snake is oriented locally

away from the center, if $\Phi = +1$,

towards the center, if $\Phi = -1$.

The center was called a source or sink, accordingly. By [Fiedler] (1986 b),

$$\sum_S \Phi = 0 \tag{4.6}$$

along the Jordan curve S, since the interior of S does not contain any B-points. In other words, the number of sources equals the number of sinks, as far as Hopf bifurcation is concerned.

We establish an analogous result for bifurcation from tame homoclinic orbits on S next. Let $\tilde{\lambda}_j$ enumerate the intersection points with S of the oriented tame homoclinic paths γ_m near the stratified loop $\{\lambda^*\} \times H^*$. Let $i_j = \pm 1$ denote the local intersection index, at $\lambda = \lambda_j$, of the positively oriented smooth closed Jordan curve S with the oriented tame homoclinic path γ_m. In other words, $i_j = +1$ if the tangent vectors of S and γ_m, in this order and

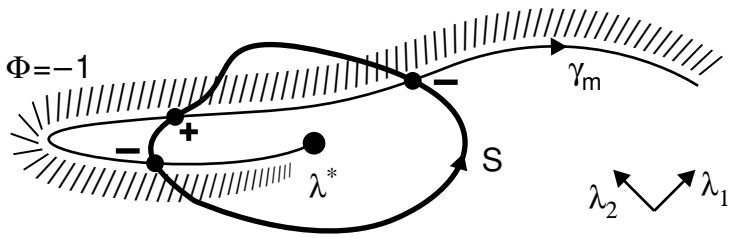

Figure 4.2: The intersection indices i_j of S with γ_m.

along the given orientations, are a positively oriented pair. Define $i_j = -1$ otherwise; see figure 4.2. Define $i(\gamma_m) = +1$, if γ_m is oriented towards λ^*, and $i(\gamma_m) = -1$ otherwise. Using $i(\gamma_m)$ we can rewrite our claim (4.4) as

$$\sum_m i(\gamma_m) = 0. \tag{4.7}$$

Also note that for any fixed m

$$\sum_{\lambda_j \in \gamma_m} i_j = i(\gamma_m), \tag{4.8}$$

as in figure 4.2, by homotopy invariance with respect to γ_m. Thus it is sufficient to show

$$\sum_j i_j = 0, \tag{4.9}$$

where the sum over j now enumerates all intersection points $\tilde{\lambda}_j$ of all the homoclinic paths γ_m with S.

Our proof of (4.9) is indirect: suppose

$$\sum_j i_j \neq 0. \tag{4.10}$$

Recall the generic approximation $g_n \to f$. Since tame homoclinic paths remain tame, under this approximation, and since the tame paths γ_m intersect S transversely, the intersection points $\tilde{\lambda}_j$ and their homoclinic orbits h_j are slightly perturbed for g_n to become

$$\tilde{\lambda}_{j,n} \to \tilde{\lambda}_j \ ,$$
$$h_{j,n} \to h_j \ .$$

In particular, the intersection indices i_j, the orientations of the paths $\gamma_{m,n} \to \gamma_m$, and the orbit indices Φ of the per sheet accompanying γ_m remain unchanged along S. Therefore we can assume that (4.10) holds for all g_n.

Consider the snakes of periodic orbits along S, generated at the intersections $(\tilde{\lambda}_{j,n}, h_{j,n})$. We claim that the snake generated at $h_{j,n}$ is oriented

away from $(\tilde{\lambda}_{j,n}, h_{j,n})$ if $i_j = +1$,
towards $(\tilde{\lambda}_{j,n}, h_{j,n})$ if $i_j = -1$.

In other words, $i_j = +1$ is a source of a snake whereas $i_j = -1$ is a sink (at the limit of infinite period of the periodic solutions in the snake).

To prove the above claim, first recall that i_j is the local intersection index of S with γ_m (we omit the additional subscript n, for the moment). The snake, secondly, is oriented along S, for $\Phi = +1$, and anti S, for $\Phi = -1$. Thirdly, the orientation of γ_m is related to Φ, by definition 3.1, as follows. (For an example, see figure 4.2 again). Consider the ordered pair at $\tilde{\lambda}_j$, given by the tangent vector to S, pointing to the side of the per sheet, and the tangent vector to γ_m, along its orientation. This ordered pair has orientation $\Phi = \pm 1$. Using the tangent vector to S along its (positive) orientation, instead, the orientation of the same pair is i_j. Thus the per sheet bifurcates in the direction of the positive orientation of S if $i_j \cdot \Phi = +1$, and in the negative direction if $i_j \cdot \Phi = -1$. In particular, $i_j = +1$ is a source and $i_j = -1$ is a sink of a snake at infinite period.

In view of (4.10), the number of sources of snakes differs from the number of sinks, at infinite period and in $S \times V_x$.

Since $\sum \Phi = 0$, by (4.6), this imbalance remains in effect if centers are taken into account as sources and sinks of snakes at finite period. Therefore, for

any small $\delta > 0$ there must exist a *global snake* $\mathfrak{S}_n$ of g_n along S: a snake which

(4.11.a) touches the boundary of V_x, or

(4.11.b) contains points, at a distance at least δ from the homoclinic orbits, which lie on periodic orbits of arbitrarily large minimal period.

By construction the snake $\mathfrak{S}_n$ bifurcates at a tame homoclinic orbit or at a Hopf bifurcation point. Note that δ can be chosen independently of n, because tameness of homoclinic orbits persists.

Passing to the limit $n \to \infty, g_n \to f$, we will obtain a contradiction, thereby proving our original claims (4.4), (4.7), (4.9). Indeed, $\mathfrak{S}_n$ limits onto a continuum $\mathfrak{S}$ of periodic orbits in $S \times V_x$ such that (4.11.a,b) remain valid if we replace "minimal period" by *virtual period*. For a proof see [Fiedler] (1985), [Fiedler, chapter 7] (1988). We now recall that $\{\lambda^*\} \times H^*$ is assumed to be stratified; in particular definition 2.11 (ii) holds for $\mathcal{C} := \mathfrak{S}$. Hence $\mathfrak{S}$ cannot touch the boundary of V_x as in (4.11.a). Therefore, (4.11.b) applies: $\mathfrak{S}$ must contain periodic orbits of arbitrarily large virtual periods at a distance at least δ from the homoclinic orbits. This clearly contradicts definition 2.11 (ii), where convergence of a subsequence to a homoclinic orbit is required.

This contradiction completes the indirect proof of the lemma, and the proof of theorem 3.4. □

5 More examples

In this section we illustrate scope and limitations of our pathfollowing approach by eight additional examples. Examples 5.1 – 5.3 consider stratified loops, example 5.3 showing some global interaction in local unfoldings of certain codimension three degenerate planar vector fields. The remaining examples 5.4 – 5.8 address the issue of non-stratified loops and chaotic dynamics, including the Belyakov transitions to the Shilnikov region, 5.4, and the Lorenz homoclinic explosion, 5.8.

5.1 Example: fold hitting

Locally at a nondegenerate stationary fold point (λ, x), the stable set $W^s(\lambda)$ is an immersed manifold with boundary given by $W^{ss}(\lambda)$, the strong stable manifold. Similarly, the local unstable set $W^u(\lambda)$ has the strong unstable manifold $W^{uu}(\lambda)$ as a boundary. Denoting the respective dimensions by $s, ss, \ldots$, we have

$$ss + 1 = s,$$
$$uu + 1 = u,$$
$$s + u = N + 1,$$

where $N = \dim X$ is the dimension of the phase space. We have already observed in example 2.7 that a homoclinic path can, even generically, coincide with a fold. This occurs when $W^s(\lambda)$ and $W^u(\lambda)$ intersect transversely (and not on a boundary). Moving (λ, x) along the fold curve in two parameters, such a transverse intersection can disappear, for example, by $W^s(\lambda)$ sliding across the boundary $W^{uu}(\lambda)$ of $W^u(\lambda)$, at $\lambda = \lambda^*$ and at an associated loop

$$H^* = \mathrm{clos}(W^s(\lambda^*) \cap W^{uu}(\lambda^*)).$$

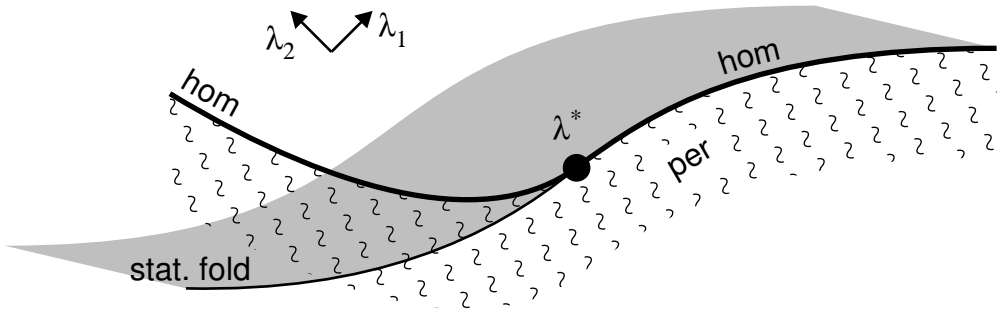

Figure 5.1: The fold hitting.

Under generic nondegeneracy assumptions, it turns out that a homoclinic path persists but detaches from the fold at $\lambda = \lambda^*$. Tracking the hom path in the opposite direction we call the homoclinic bifurcation at $\lambda = \lambda^*$ a *fold hitting*. This bifurcation was first investigated by [Lukyanov] (1982), in the plane. [Schecter] (1987 a,b) gives a revised account and an application to the Josephson junction. For a detailed analysis in $\mathbb{R}^N$ see [Chow & Lin] (1990) and [Deng] (1990). For the bifurcation diagram see figure 5.1.

It turns out that the hom path is accompanied by a unique sheet of uniformly hyperbolic periodic orbits. In particular the hom path is tame. If the periodic orbits have nonzero orbit index Φ, then the tame path is oriented accordingly, consistently through the stratified homoclinic loop $\{\lambda^*\} \times H^*$.

Let us augment this example, assuming that, at the hitting value $\lambda = \lambda^*$, there exists still another homoclinic orbit to the fold via another transverse intersection $W^u(\lambda^*) \cap W^s(\lambda^*)$, not on the boundary. This requires $\dim X \geq 3$. While the original hom path γ_1 detaches from the stationary fold, the transverse intersection generates a second path γ_2 which stays on the fold. By [Shilnikov] (1969), shift dynamics on two symbols occurs near the homoclinic paths γ_1, γ_2 where they both stick to the fold. The two symbols 1, 2 indicate

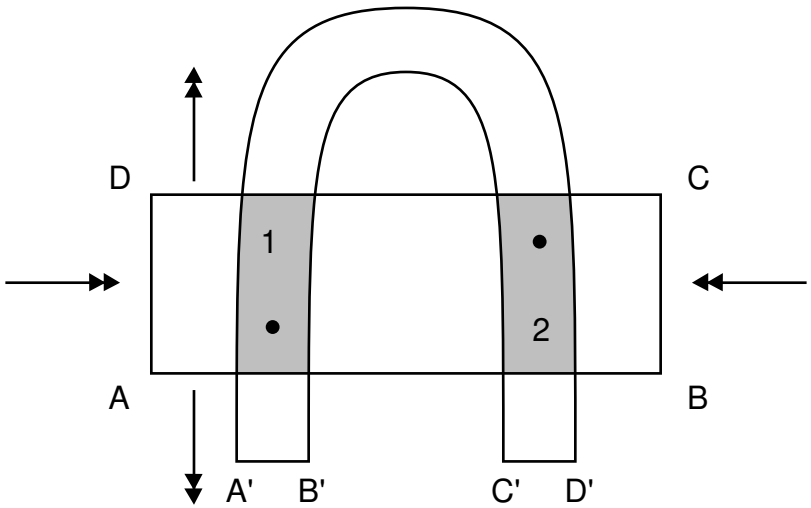

Figure 5.2: Fixed points in the horseshoe.

excursions along the original homoclinic orbits of γ_1, γ_2, respectively, which occur beyond the fold curve, where the stationary points have annihilated. In spite of this chaotic dynamics, note that each of the paths γ_1, γ_2 will be tame, separately, because the shift type orbits necessarily leave a neighborhood of each. In effect, homoclinic pathfollowing can remain an option, even in the presence of chaotic dynamics.

Following γ_1, γ_2 further, along the fold and away from λ^*, we may also consider their subsequent annihilation: the respective transverse intersections $W^s(\lambda) \cap W^u(\lambda)$ approach each other and disappear at a non-transverse interior intersection $\{\tilde{\lambda}\} \times \tilde{H}$. Although pathfollowing through $\{\tilde{\lambda}\} \times \tilde{H}$ seems obvious, joining the paths γ_1 and γ_2, we do not expect $\{\tilde{\lambda}\} \times \tilde{H}$ to be stratified. In fact, note that near λ^* the periodic orbits generated from γ_1, γ_2, with corresponding trivial sequences $\mathbf{1} = \ldots 111 \ldots$, $\mathbf{2} = \ldots 222 \ldots$, respectively, are both hyperbolic with equal unstable dimensions, due to the hyperbolic structure of the Smale horseshoe in which they must occur. Due to sub-

sequent annihilation at $\tilde{\lambda}$, the geometry of the Poincaré map near λ^* is as indicated in figure 5.2 for $\dim X = 3$. In particular, note that $\Phi = -1$ at the fixed point **1** whereas $\Phi = 0$ at **2**. Therefore, only γ_1 will be oriented. (In fact, a similar reasoning applies to all periodic orbits in the horseshoe: again $\Phi \in \{-1, 0\}$). In particular, Lemma 4.1 fails at $\{\tilde{\lambda}\} \times \tilde{H}$. Therefore $\{\tilde{\lambda}\} \times \tilde{H}$ cannot be stratified. Moreover γ_1 does not continue into the non-oriented tame path γ_2, all the way back to λ^*. Instead, we expect further non-stratified loops or a cascade of (non-resonant) homoclinic doublings to occur.

5.2 Example: bi-contractive het loop

A heteroclinic loop consists, in the simplest case, of a pair of distinct equilibria A, B and a pair AB, BA of heteroclinic orbits joining them, from A to B and vice versa, respectively. With slight adaptations, we follow [Chow et al.] (1990 b, 1991), [Deng] (1991 a,b) who also give applications to travelling waves of the FitzHugh-Nagumo system. We assume that A, B are both hyperbolic, only one-dimensionally unstable, the principal stable eigenvalue μ_- is simple real (as the (principal) unstable eigenvalue μ_+), the heteroclinic orbits limit tangentially to the associated principal eigenvectors, and each equilibrium is locally contractive:

$$\begin{aligned} &\mu_-(A) + \mu_+(A) < 0, \\ &\mu_-(B) + \mu_+(B) < 0. \end{aligned} \tag{5.1}$$

Under these assumptions and canonical transversality conditions with respect to parameter dependence of the stable and unstable manifolds, the bifurcation diagrams in figures 5.3 – 5.5 were established, see [Deng] (1991 a). Figures 5.3 and 5.5 can be realized by planar vector fields.

The three cases in figures 5.3 – 5.5 differ by a global twist condition along the

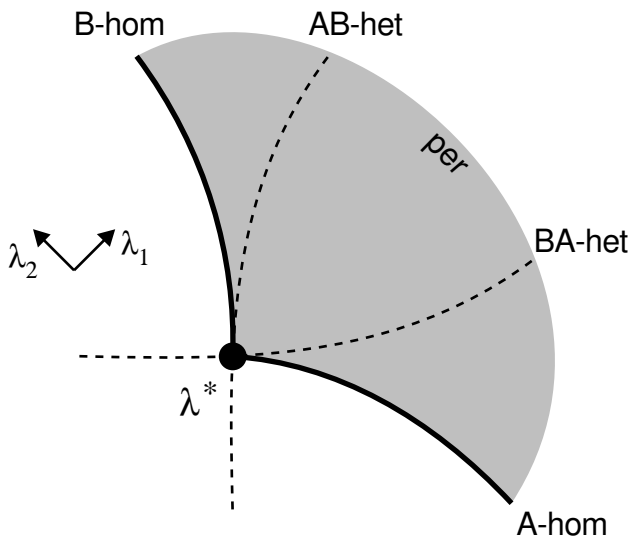

Figure 5.3: Bi-contractive het loop, no twist.

heteroclinic orbits AB and BA. Geometrically, the twist arises by collapsing the fibers of the associated strong stable foliation with contraction rates exceeding $\mu_-(A), \mu_-(B)$, locally. Then the het loop occurs within a two-dimensional annulus, each half of which may be twisted or not. The non-twisted and the doubly twisted case, figures 5.3 and 5.5, provide an orientable annulus and thus can occur in the plane. One twist, alias the Möbius band, requires at least $X = \mathbb{R}^3$ for an embeeding.

In all three cases, we note the two het paths crossing at the bifurcation point $\lambda = \lambda^*$. Moreover, two hom paths emanate from λ^*, one for each associated equilibrium A, B. Also note the additional $ABAB$ het path in figure 5.4 and, in figure 5.5, the sequences of heteroclinic bifurcation curves $(AB)^k, (BA)^k$, $k = 1, 2, 3, \ldots$ of orbits which pass near A, B successively, $k-1$ times, before converging to A or B. In all three cases, there is a unique sheet of hyperbolic periodic orbits extending from the A-hom path to the B-hom path. Both hom

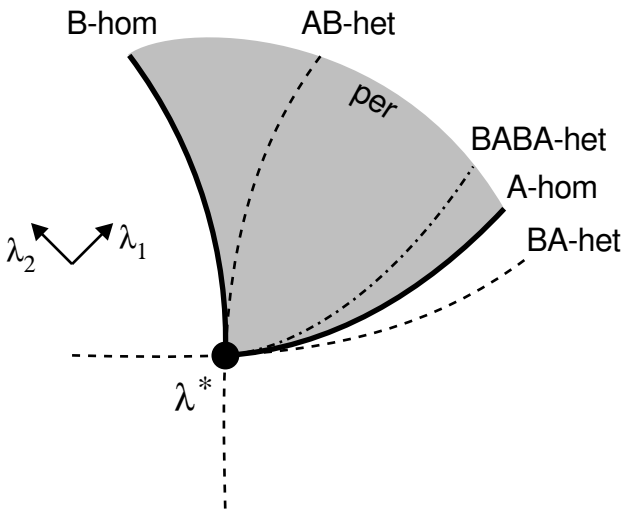

Figure 5.4: Bi-contractive het loop, one twist.

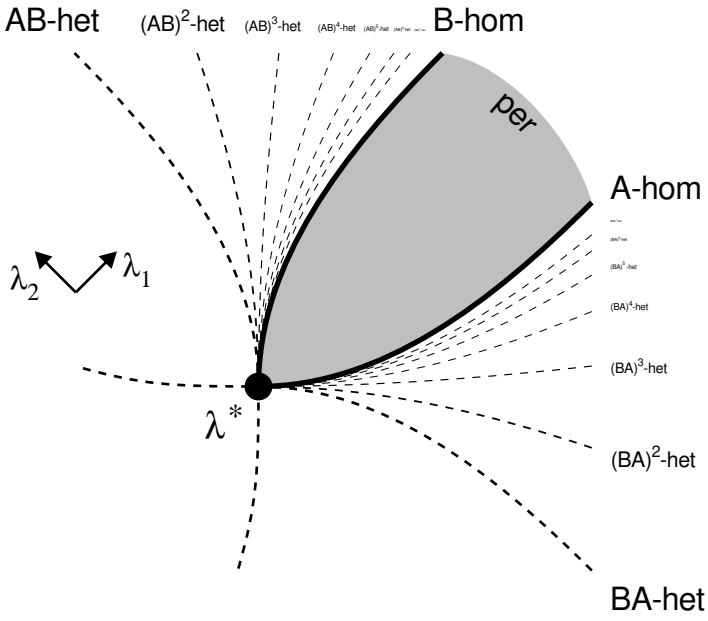

Figure 5.5: Bi-contractive het loop, double twist.

paths are therefore tame, in each case, and the corresponding het loops are stratified. The same holds true, if the unstable dimensions of the equilibria A, B exceed one but remain equal. Seeing this, however, requires a center manifold reduction which we cannot indicate here.

5.3 Example: codimension three unfoldings

Following [Dumortier et al.] (1991), we consider the three parameter family of planar vector fields

$$(5.2)\qquad \begin{aligned} \dot{x}_1 &= x_2 \\ \dot{x}_2 &= \lambda_1 + \lambda_2 x_1 + a x_1^3 + x_2(\lambda_3 + b x_1 + x_1^2). \end{aligned}$$

with small real unfolding parameters $\lambda_1, \lambda_2, \lambda_3$ and constant coefficients $a = \pm 1, b > 0, b \neq 2\sqrt{2}$. For λ, x in a neighborhood of zero, the vector field describes coalescence of two B-points of opposite B-index. See also [Medved] (1985).

To describe the flow of (5.2), we restrict the parameters λ to a small sphere centered at the origin; removing the north pole, three planar bifurcation diagrams are obtained. All three diagrams turn out to be essentially independent of the (small) radius of the sphere in parameter space. We sketch the three cases in rudimentary form as figures 5.6 – 5.8. They were called saddle, focus, and elliptic to distinguish the behavior of the degenerate germ at $\lambda = 0, x = 0$. The notation (u) or (u_1, u_2, u_3) again indicates unstable dimensions of hyperbolic equilibria.

We illustrate consistency of these diagrams with our global pathfollowing approach. We consider figure 5.6 first, in some detail. Outside the cusped oval, there is a unique steady state. The steady state is a saddle: hence no homoclinic or periodic recurrence. Inside the oval, three steady states coexist, all generated by saddle-node bifurcations on the fold line. One of

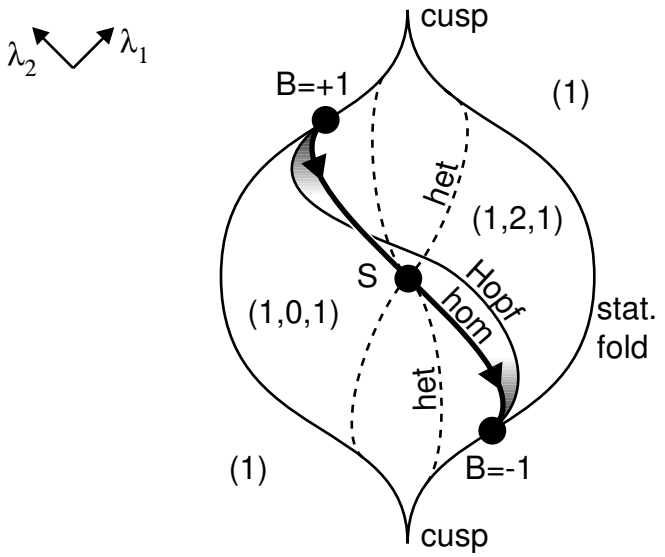

Figure 5.6: Codimension three, saddle, $a = 1$.

them undergoes Hopf bifurcation, becoming a local attractor, (0), or repeller, (2), on the respective sides of the Hopf path. The Hopf path itself joins two B-points of opposite B-index, computable from (3.4). As usual, each B-point in turn generates a local tame oriented hom path. Note that these local paths are associated to different saddles inside the cusped oval, which are not related by stationary continuation inside the cusped oval. In the $(1, u_2, 1)$ notation for unstable dimensions, the local hom paths are associated to the first and last entry, respectively, since $u_2 \in \{0, 2\}$ denotes an attractor or repeller. Assume genericity of the two-parameter family and uniform boundedness of the hom paths next. Then the local hom paths have to join, globally, for these planar vector fields. The necessary exchange of associated equilibria can happen only via at least one stratified heteroclinic loop. In figure 5.6 this stratified bifurcation point is denoted by S. Detailed analysis

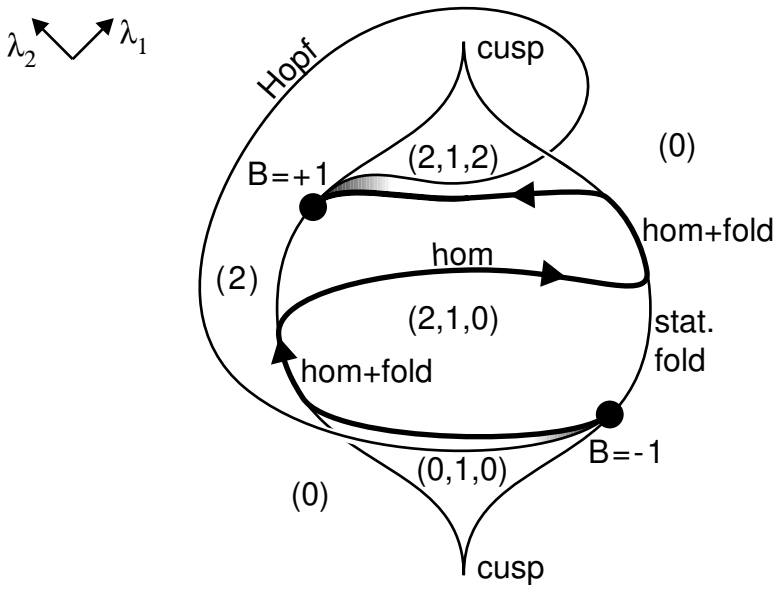

Figure 5.7: Codimension three, focus, $a = -1,\ 0 < b < 2\sqrt{2}$.

by [Dumortier et al.] (1991) shows that the het loop at S is not bi-contractive, and example 5.2 does not provide the correct local bifurcation diagram at S. Besides a tame hom path and two het paths, AB and BA, through S, a per fold also terminates there. The het paths from S hit the stationary fold and persist there. Since S is stratified, the hom path can be oriented consistently through S. With the hom path oriented successfully, note that the accompanying per sheet lies on opposite sides, near the two B-points. Alternatively, note that the periodic orbits are stable near $B = -1$, but unstable near $B = +1$, in the present case. The switching is achieved via the (omitted) per fold, originating at the Hopf path and terminating at S.

We briefly discuss figures 5.7, 5.8 next. In figure 5.7, the Hopf path connects the B-points via the exterior region of the cusped oval. The local hom paths are trapped inside the oval, both associated to the second entry in $(u_1, 1, u_3)$,

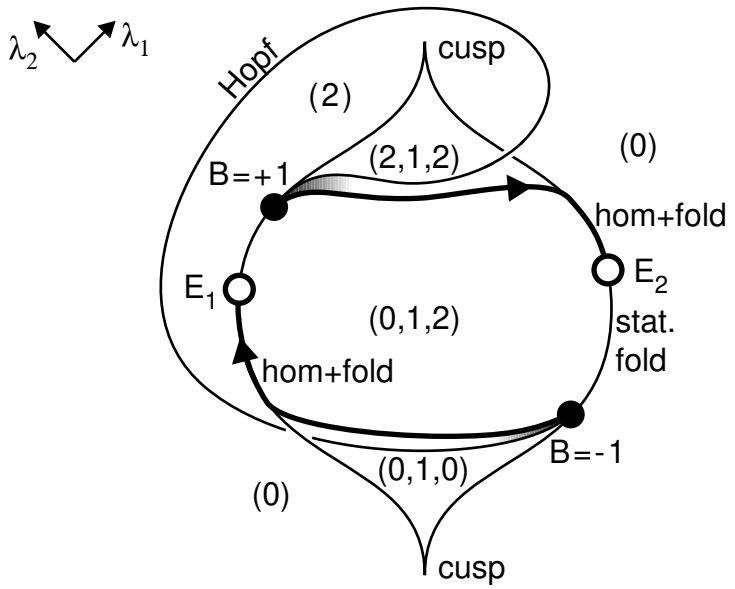

Figure 5.8: Codimension three, elliptic $a = -1,\ b > 2\sqrt{2}$.

because $u_1, u_3 \in \{0, 2\}$ indicate local attractors or repellers. The local hom paths remain bounded, thus joining up to a single hom path with consistent orientation. It turns out, due to planar phase plane geometry, that the global oriented hom path hits/leaves the stationary fold curves at four stratified fold hitting bifurcations as discussed in example 5.1. Again the per sheets lie on opposite sides of the oriented hom path, near the two B-points. Therefore, resonant homoclinic side switching as in example 2.9 (a) must also occur here. Recall that this involves an exponentially flat bifurcation of a periodic saddle-node curve from the hom path.

In figure 5.8, finally, each local hom path hits the fold curves as in example 5.1. At E_1, E_2 the hom paths escape to infinity, leaving in particular the neighborhood of validity of the unfolding. This illustrates yet another option of theorem 3.4 and remark 3.5 (iii).

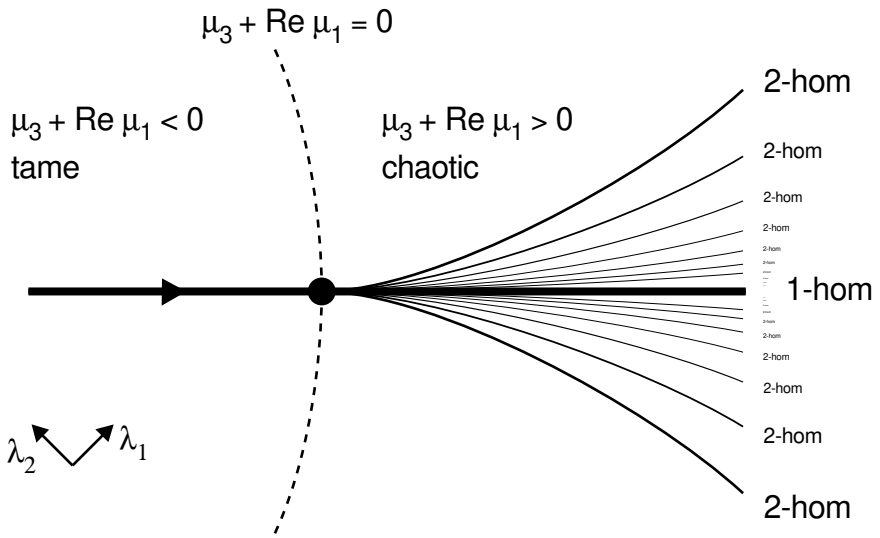

Figure 5.9: Resonant Belyakov transition.

5.4 Example: Belyakov transitions

[Belyakov] (1980, 1984) has investigated tame hom paths transgressing into the Shilnikov chaotic region. His results are very illuminating, and at the same time slightly discouraging from a global pathfollowing point of view. Expressed in terms of the eigenvalues μ_j of the associated equilibrium in $X = \mathbb{R}^3$ the two transitions are

a) originally, $0 < -\mu_1 < -\mu_2 < \mu_3$, and then μ_1, μ_2 join up, becoming conjugate complex, $0 < -Re\mu_1 = -Re\mu_2 < \mu_3$;

b) throughout $Re\mu_1 = Re\mu_2 < 0 < \mu_3$ with a complex pair $\mu_2 = \overline{\mu}_1$, and $\mu_3 + Re\mu_1$ changes sign.

A partial bifurcation diagram of the resonant case b) showing only 1-hom and 2-hom paths is given in figure 5.9; see [Belyakov] (1984). Clearly, the

transition b) is not stratified, since infinitely many 2-hom branches accumulate at the bifurcation point. A similar statement holds for case a). But even if we are willing to lay definitions aside, for a moment, it is not clear at all how we should continue, if we happen to approach the transition point from within the chaotic region, following one of the 2-hom paths. Therefore, we stop the pathfollowing process, in theorem 3.4, as soon as a hom path reaches the boundary of the chaotic region.

5.5 Example: the fold-Hopf, revisited

We return to examples 2.7 (a), (b) with pathfollowing in mind. Consider case (a), figures 2.2 (a) and 2.3, first. Note that the fold-Hopf at $\lambda = 0, x = 0$ may be stratified in that case. Indeed suppose the orbits with α- and ω-limit set given by the origin form an isolated invariant set with isolating neighborhood V_x in the sense of [Conley] (1978). Then V_x also contains the fold-hom path, for small $|\lambda|$. A small circle S around $\lambda = 0$ in parameter space will provide the two hom orbits on the fold, in V_x, but no further homoclinic orbits. Moreover, periodic orbits in V_x cannot touch the boundary of the isolating neighborhood V_x. Small periodic orbits are generated at the two Hopf points on S. Large periodic orbits are generated at the two homoclinic orbits on S. The large periodic orbits just inter-connect the two homoclinic orbits along S. Choosing S such that the torus bifurcation for $\lambda_2 < 0$ occurs at irrational rotation number, the small periodic orbits just inter-connect the two Hopf points on S. This then proves that the fold-Hopf loop is stratified. In particular, the orientation of the hom paths along the fold extends consistently through the fold-Hopf loop. (Note that the orbit index Φ does not change at the torus bifurcation).

The other case, 2.7 (b), is less innocent. We have already mentioned that,

breaking S^1-equivariance of the normal form, shift dynamics can occur, even at $\lambda = 0$. Above the Hopf curve of figure 2.3, a periodic saddle with transverse intersections between stable and unstable manifolds can exist. Strictly speaking, however, shift dynamics could occur even near a stratified loop. Still, similarly to our augmented example 5.1, we do not expect the fold-Hopf 2.7 (b) to be stratified with such complicated dynamics nearby.

5.6 Example: Bykov's semi-robust het loop

We indicate a two-parameter example in $X = \mathbb{R}^3$ investigated by [Bykov] (1978, 1980, 1988). We are indebted to V. Afraimovich for this reference. As in the bi-contractive case of example 5.2 consider a pair A, B of distinct hyperbolic equilibria joined by a pair AB, BA of heteroclinic orbits at parameter $\lambda = 0$. Again suppose that B is one-dimensionally unstable with real eigenvalues $\mu_+(B) > 0 > \mu_-(B) > \mu_{--}(B)$ and AB approaches B along the principal eigendirection of $\mu_-(B)$. Deviating from example 5.2, however, assume that B is expansive,

$$\mu_-(B) + \mu_+(B) > 0, \tag{5.3}$$

and that the unstable dimension of A is two, differing from the unstable dimension of B. Under the usual nondegeneracy assumptions, this implies that the heteroclinic orbit $AB(\lambda)$ from A to B persists under small perturbations of λ. In contrast, BA immediately disappears for $\lambda \neq 0$. We therefore call the het loop *semi-robust*.

Following Bykov, we finally assume $\mu_-(A) < 0$ is real and $\mu_+(A)$ form a complex pair with

$$\mu_-(A) + Re\mu_+(A) > 0. \tag{5.4}$$

Note that an A-hom can be tame in that case; we are not in the situation of

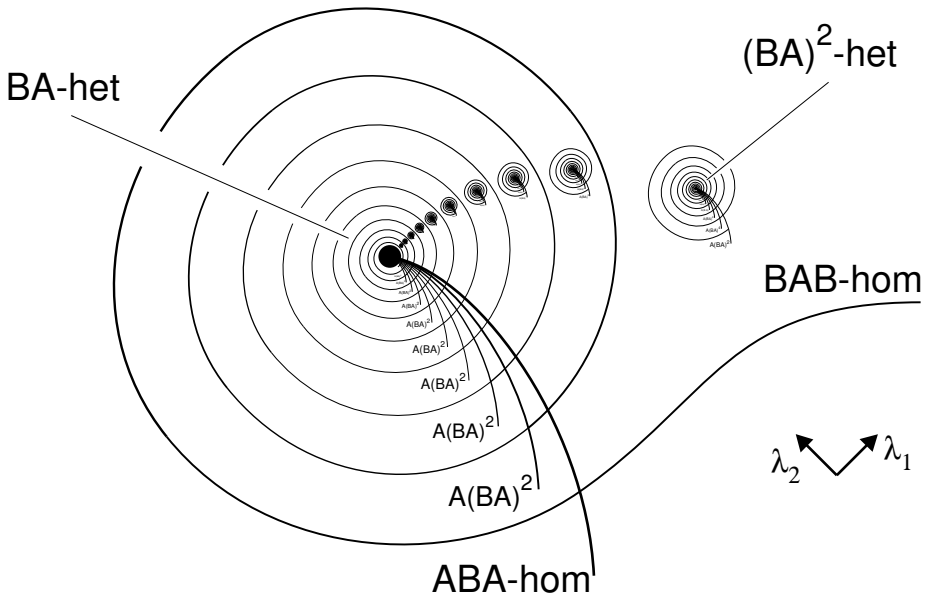

Figure 5.10: A semi-robust het loop.

Shilnikov chaos.

A partial bifurcation diagram was given in [Bykov] (1978); for some aspects see figure 5.10. For a more complete, detailed, and complicated description see [Bykov] (1980, 1988). Descriptively, there is a logarithmic spiral BAB towards $\lambda = 0$ where B-hom orbits exist which pass near A once. Also there is a non-spiraling curve ABA of A-hom orbits which pass near B once. Note that each of these homoclinic paths is tame in our setting, separately, except that the twist type may change due to (omitted) bifurcations.

Besides the path of ABA-hom orbits, cycling through the het loop once, there is also a sequence of paths of $A(BA)^2$-hom orbits which cycle through the het loop twice. By this fact alone, Bykov's het loop is not stratified.

Similarly to Tresser's 8, a selfsimilarity is present. In fact, there is a sequence of $(BA)^2$ heteroclinic orbits at $\lambda = \lambda_m$, accumulating to the original het

loop at $\lambda = 0$ for $m \to \infty$. Since the AB heteroclinic orbit persists, near $\lambda = 0$, this implies that the entire bifurcation scenario repeats near each λ_m, including sequences $\lambda_{m,m'} \to \lambda_m$ for $m' \to \infty$, replacing the sequence λ_m, and so forth. Clearly, Bykov's het loop is not stratified in any neighborhood.

The case when (5.4) is replaced by the opposite inequality

(5.5) $\qquad \mu_-(A) + Re\mu_+(A) < 0$

has been analyzed by [Kokubu] (1990, 1991) in an AB-het, BC-het, AC-het context. He obtains the ABA and BAB hom paths and points out Shilnikov chaos along the ABA hom path.

5.7 Example: tame 8, doubly twisted real saddle

Following [Gambaudo] (1987), we consider a real variant of Tresser's tame 8 from example 2.10. Again two tame hom paths cross each other transversely, as in figure 2.6(b). But this time it is assumed that all eigenvalues at the associated equilibrium A are real, and the two homoclinic orbits form a figure 8 following the simple principal eigendirections from respectively opposite sides. To utilize a foliation argument in [Gambaudo] (1987), the unstable dimension of A is assumed to be one. Moreover, contractivity

(5.6) $\qquad \mu_-(A) + \mu_+(A) < 0$

is assumed for the principal eigenvalues $\mu_\pm(A)$. Standard nondegeneracy conditions are also imposed. Collapsing strong stable fibers associated to the rapidly contracting non-principal stable eigendirections, the flow near each homoclinic orbit can be viewed as a flow on a two-dimensional annulus. We assume a double twist, that is, each annulus is in fact a Möbius strip.

Labeling excursions along the two homoclinic orbits by $+, -$, as in example 2.10, the hom bifurcation diagram of figure 5.11 emerges. The diagram fol-

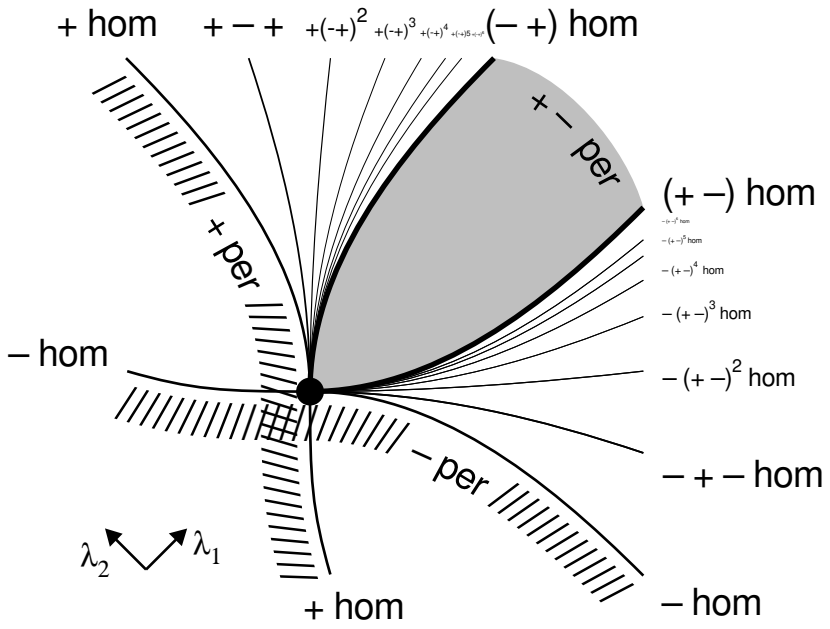

Figure 5.11: Bifurcation diagram of a doubly twisted, real saddle 8.

lows from an analysis of one-dimensional return maps on the doubly twisted double annulus. Most periodic sheets are omitted here. Note the tame +hom and −hom paths and the additional $(+-)$hom, $(-+)$hom, $+(-+)^k$hom, and $-(+-)^k$hom half-branches.

In fact the bifurcation diagram coincides with figure 5.5, replacing AB-het by +hom, BA-het by −hom, B-hom by −+hom, A-hom by +−hom, $(AB)^k$-het by $+(-+)^{k-1}$hom, and $(BA)^k$-het by $-(+-)^{k-1}$hom. To understand this "coincidence", see figure 5.12 where a figure 8 saddle is artificially split into two equilibria A, B along the dotted line. Clearly, the above correspondences can be read off from figure 5.12. Note, however, that +per and −per orbits, for example, become invisible in figure 5.12, in contrast to +−per orbits.

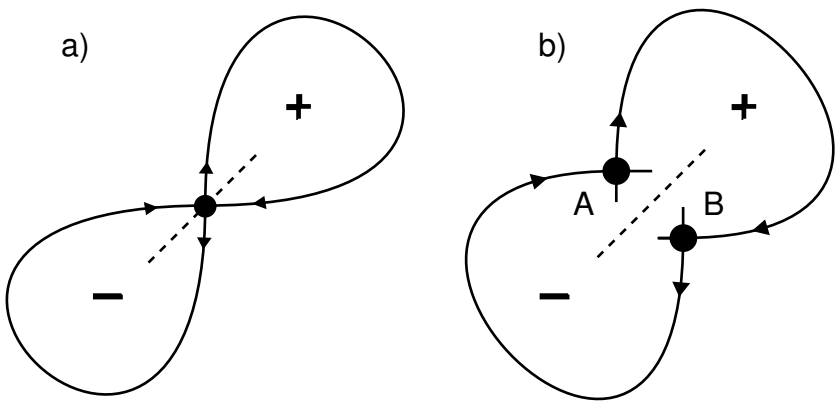

Figure 5.12: Homoclinic 8 and heteroclinic loops.

In particular, we conclude that the doubly twisted real contractive 8 is not stratified in a neighborhood of the figure 8 because infinitely many tame oriented hom paths of type $+(-+)^n, -(+-)^n$, $n = 1, 2, 3, \ldots$ bifurcate. For $n \to \infty$, the first of these families accumulates to the $-+$hom path, and the second to the $+-$hom path. Nevertheless, each of the generating $+$hom and $-$hom paths is tame and oriented, separately. Also, we see that bifurcations of periodic orbits must occur since the periodic orbits generated by the $+(-+)^n$ hom family have different winding type, containing a $++$ pair, than those of the $-(+-)^n$ family which contain a $--$ pair.

By the exact same correspondence, the bifurcation diagram of the non-twisted contractive real 8 follows from the corresponding bifurcation diagram 5.3 of the non-twisted bi-contractive het loop. In fact we again have to replace, in figure 5.3, AB-het by $+$hom, BA-het by $-$hom, B-hom by $-+$hom, A-hom by $+-$hom paths, and the per sheet by $+-$per. Only the $+$per and $-$per sheets are then omitted in figure 5.3; they extend to the left of the original AB-het and below the BA-het curves, respectively.

A similar correspondence finally holds for the bifurcation diagrams of a het

loop and a homoclinic 8 with a single twist, respectively.

In summary, we have seen how a stratified het loop, figure 5.5, instigates a homoclinic 8 to be non-stratified, figure 5.11, under a slight change of view point.

5.8 Example: tame butterfly, real saddle

Following [Gambaudo] (1987) again, we consider a double homoclinic loop to a real saddle A in $\mathbb{R}^3$. All assumptions and notations are as in example 5.7, except for the asymptotic behavior of the two homoclinic loops $h_+(t), h_-(t)$. For $t \to -\infty$, $h_+(t)$ and $h_-(t)$ are still assumed to approach the equilibrium along the principal unstable eigenvector, from opposite sides. For $t \to +\infty$, however, we assume $h_\pm(t)$ to approach the equilibrium along the principal stable eigenvector *from the same side*, see figure 5.13. Such a configuration was called "butterfly" in [Gambaudo] (1987). Again, standard nondegeneracy conditions are imposed.

We consider the expansive case

(5.7) $\qquad \mu_-(A) + \mu_+(A) > 0$

first. We do not give a complete two-parameter bifurcation diagram. Instead, we pass to a double cover, splitting A into two copies A, B as in figure 5.14. Next we associate to the thus created het loop a flow on a (twisted or non-twisted) annulus, identifying fibers of the strong stable foliation. We consider the case where the orientations are as indicated in figure 5.14. Such a foliation was established, for example, in the geometric Lorenz model, see [Robinson] (1981). Reversing the flow in the annulus, the results of example 5.2 apply. Note that the standard (i.e. non-twisted) Lorenz situation leads to a doubly twisted het loop, figure 5.5, in our case. In particular, the

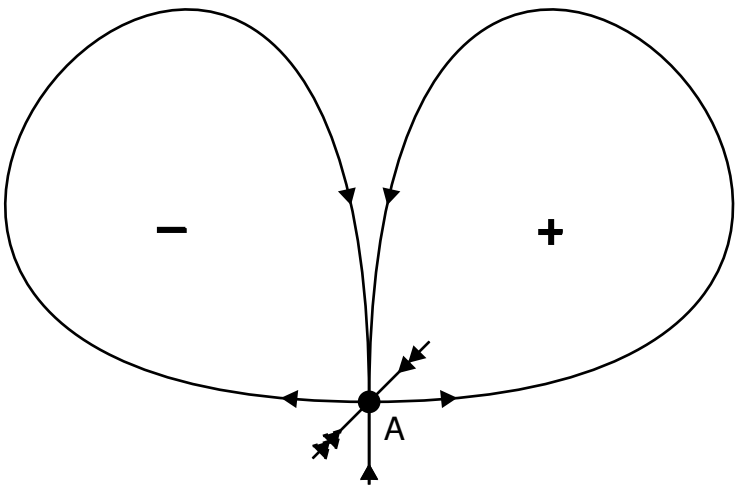

Figure 5.13: A tame butterfly.

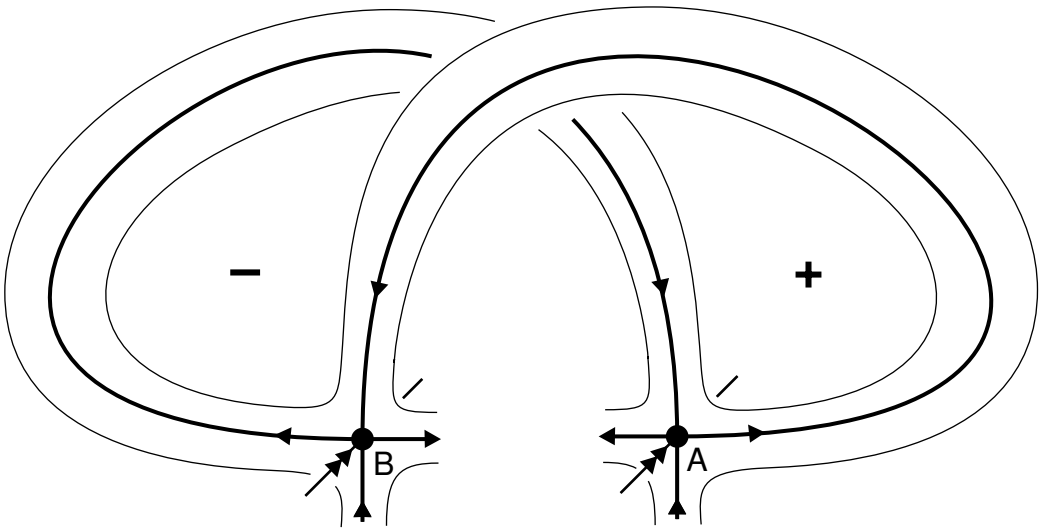

Figure 5.14: A split butterfly.

bifurcation diagram of figure 5.11 still forms a partial bifurcation diagram for the present situation. Hom branches which contain $++$ or $--$ blocks in their coding have been lost, of course, when splitting the butterfly. (So better leave the butterflies intact). But the branches found are sufficient to prove that the tame butterfly is not stratified.

The contractive case

$$\mu_-(A) + \mu_+(A) < 0, \tag{5.8}$$

also considered in [Gambaudo] (1987), can be treated analogously but without reversing the flow in the annulus.

6 Homoclinic trapping

When reviewing some examples of stratified loops, we have discussed three more global homoclinic bifurcation diagrams, in example 5.3, which can be understood in terms of stratified loops alone. In the present section, in contrast, we give two examples where global homoclinic pathfollowing runs into complicated recurrent dynamics. This conclusion will be drawn from only local information at the equilibria. The first example involves a "lip" on an S^2-isola. The second example, however, is dissipative. In both examples homoclinic paths would be trapped in certain regions of parameter space, unless non-stratified loops, chaotic dynamics, or unbounded ϵ-length were involved. We regret that we have to artificially cook up such examples, at this stage, rather than being able to just refer to the applied literature.

6.1 Example: trapped lip

Consider a generic vector field f on $\Lambda \times X, X = \mathbb{R}^4$, such that the set of bounded solutions is bounded. Let the equilibrium set be a 2-sphere isola $S^2 \subseteq \Lambda \times X$. Let the fold set on S^2 be given by the equator. Assume the fold set contains two B-points, necessarily of opposite B-index, see figure 6.1. Relating B-index and center index as above (3.11), we conclude that the Hopf paths generated at the two B-points must join up, for example as in figure 6.1. Assume that an additional Hopf path, following approximately a longitude circle, separates the two B-points. Generically, this generates at least three codimension two bifurcation points: one Hopf bifurcation with two non-resonant purely imaginary pairs, and two fold-Hopf points. In a center manifold of each fold-Hopf point, we assume the local bifurcation diagram of figure 2.3. However, we require that none of the two fold-Hopf points

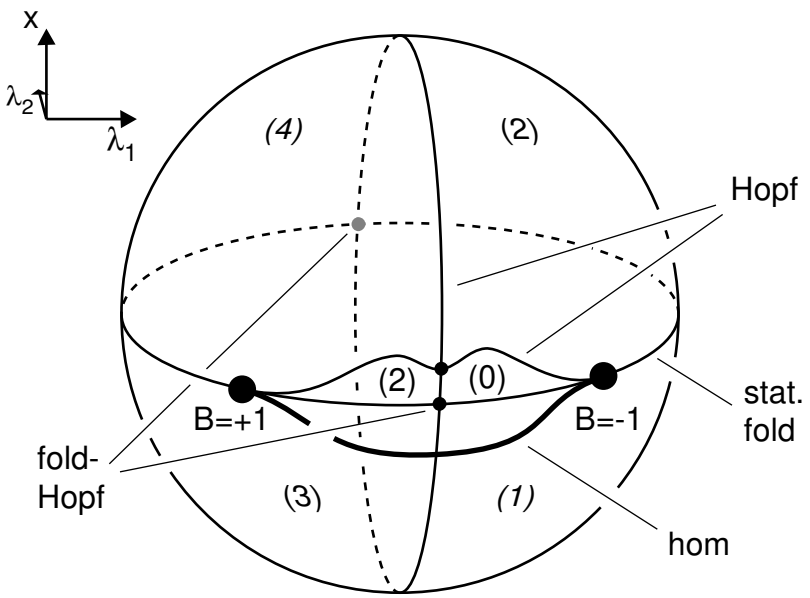

Figure 6.1: Stationary isola with B-points and separating Hopf circle. Unstable dimensions u are denoted as (u).

is part of a loop, in the sense of proposition 2.8. For the assumed global bifurcation diagram of steady states and Hopf points see figure 6.2. There are two regions of type (2,3); by (2,3)' we denote the one adjacent to the fold. In the interior (2,3) region, away from the fold, we finally assume that the four eigenvalues of the 2-dimensionally unstable "top" equilibrium form two complex pairs.

Now consider the global tame oriented hom path generated at the B-point with $B = +1$, by theorem 3.4. Because the set of bounded solutions is assumed to be bounded, this path remains bounded. We claim that the path hits a non-stratified loop, or hits the boundary of the chaotic homoclinic set, or develops unbounded ϵ-length within a bounded set. In short, complicated recurrence must occur.

We prove our claim indirectly. If none of the above occurs, then our tame

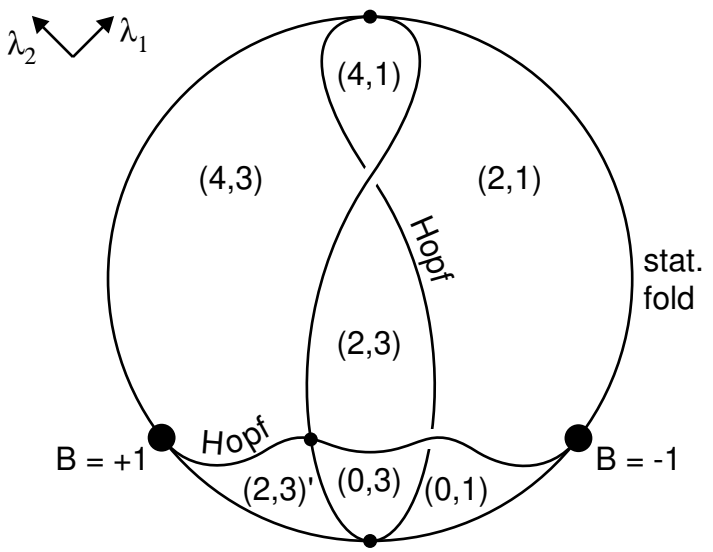

Figure 6.2: Bifurcation diagram of figure 6.1. Unstable dimensions at equilibria are denoted as (u_1, u_2).

oriented hom path must extend tamely to $B = -1$, possibly through a series of stratified het loops and fold hittings involving the upper and lower hemispheres of the stationary isola S^2. But there are "forbidden regions", which render such a path impossible.

We enumerate the "forbidden regions" next. Trivially, equilibria with unstable dimension 0 or 4, i.e. local attractors or repellers, cannot be associated to a homoclinic orbit. Each fold-Hopf point possesses a neighborhood which the hom path cannot enter, by proposition 2.8. Indeed, no fold-Hopf point is part of a loop. Moreover, neighborhoods of the Hopf paths are forbidden. Indeed, outside the already forbidden neighborhoods of fold-Hopf points we find the Shilnikov conditions for chaotic dynamics satisfied (unless we have an attractor or repeller, anyway). The top (2)-equilibrium in the interior region (2,3) away from the fold is forbidden, for a similar reason.

Now follow the tame oriented hom path generated at $B = +1$. The associated equilibrium, (3), lies in the bottom hemisphere. It can jump to the top (hemisphere), or cross the fold, but only into the (2,3)' region. Even after any such a transition, the path is trapped by forbidden regions, just as it was in the bottom hemisphere. This proves our claim.

Note that without our eigenvalue assumption on the top equilibrium in the interior (2,3) region the following itinerary of equilibria associated to a tame path would be possible:

start at $B = +1$,
(4,3) region, bottom,
(2,3) region, bottom,
(2,3) region, top, via het loop,
(2,1) region, top,
(2,1) region, bottom, via het loop or fold hittings,
terminate at $B = -1$.

Under our assumptions, this path is of course forbidden. The hom path indicated in figure 6.1 crosses the Hopf line, which induces Shilnikov chaos, and completes the trapping of the lip.

6.2 Example: dissipative trapping

The previous example cannot be dissipative, without further equilibria besides the S^2-isola, because dissipative systems must always contain an equilibrium [Hale] (1988). Here now is a dissipative example.

We do not build our dissipative example from scratch. Rather, we modify the trapped lip example. Again we work in $\Lambda \times X, X = \mathbb{R}^4$. For the global bifurcation diagram of steady states and Hopf paths see figure 6.3. Consider

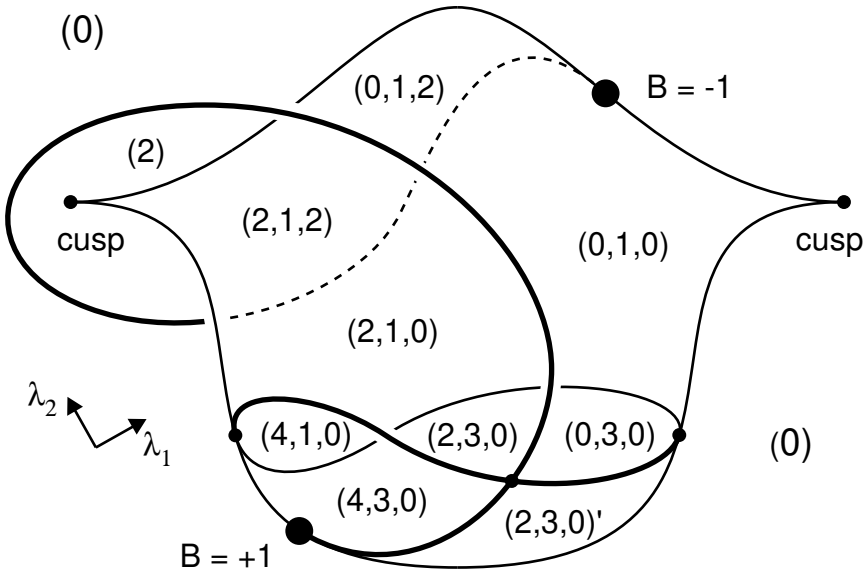

Figure 6.3: Dissipative trapping. Unstable dimensions at equilibria are denoted (u) or, "top to bottom", (u_1, u_2, u_3).

the region $\lambda_2 \leq 0$, below the λ_1-axis first. We have a sheet of stable equilibria at the "bottom". The remaining equilibria form a set equivalent to the 2-sphere S^2 of our previous example, but with a small open neighborhood of the B-point $B = -1$ removed. In particular, we make the same assumptions for these equilibria, as in the previous example. Consequently, the tame oriented hom path emanating at $B = +1$ is trapped again. Indeed, the only additional equilibrium, being a local attractor throughout, cannot interfere with trapping.

The diagram above the λ_1-axis, $\lambda_2 > 0$, indicates a completion to a globally dissipative system. Of course, the tame oriented hom path emanating, in reverse orientation, at $B = -1$ is also trapped.

Therefore both local hom paths lead to parameter regions with complicated recurrent dynamics. We emphasize that, in both examples, this conclusion could be drawn from only local information at equilibria.

7 Discussion

We will begin our discussion with a short summary, relating our examples to several aspects of our main result, theorem 3.4. We briefly address infinite-dimensional dynamical systems next. After a digression into some aspects of numerical pathfollowing of homoclinic orbits, we compare our setting with a functional analysis, boundary value problem approach on the real line and with global continuation results of Leray-Schauder type. Since we have made strong genericity assumptions, we also comment on certain important classes of vector fields with additional "non-generic" structure, specifically on Hamiltonian vector fields, time reversibility, and group equivariance. We postpone a discussion of length, ϵ-length, and topologies for the real line boundary value problem up to that point. Returning to our original setting, we then briefly review our results as an attempt of approaching, and possibly crossing, the boundary of the set of Morse-Smale systems. After some final (self-)criticism of certain inadequacies of our attempt at global homoclinic pathfollowing, we hastily conclude that our present results will only improve with any future work by the reader.

Recall our main result, theorem 3.4. Stated loosely, as in remark 3.5(0), a bounded tame oriented hom path emanating at a B-point with $B = +1$ faces the following alternative, globally. Either the path terminates at a $B = -1$ point, or else it eventually encounters complicated recurrent dynamics. For the first possibility see example 5.3.

The second alternative further splits into three cases. First, the hom path may hit a non-stratified loop. For examples see 2.10 and 5.5 – 5.8. Second, the hom path may reach the boundary of the set of chaotic homoclinic orbits. For examples see the Belyakov transitions 5.4. Third, ϵ-length may become unbounded, even though hom orbits and parameters remain uniformly

bounded in $\Lambda \times X$.

We did not give an example for the third case above. In a way, this case is analogous to minimal period becoming unbounded along a bounded continuum of periodic orbits which stays away from equilibria. In fact, the "flow plug" construction, [Harrison & Yorke] (1983), manages to interrupt orbits by trapping them within a small cross-sectional box, by a smooth flow provided $\dim X \geq 4$. For $\dim X = 3$ the problem is related to counterexamples to the so-called "Seifert conjecture": constructing vector fields on S^3 without stationary points or periodic orbits. Such counterexamples were constructed by [Schweitzer] (1974) and [Harrison] (1988), of class C^1, C^2, respectively. They are relevant for global continuation of periodic orbits, see [Alexander & Yorke] (1978), and similarly for blow-up of ϵ-length along global paths of homoclinic orbits.

Another very illuminating example related to the third case was studied by [Afraimovich & Shilnikov] (1974), [Afraimovich & Shereshevsky] (1991) in the context of boundaries of Morse-Smale systems. Consider an orbit $\tilde{h}$ which is homoclinic to a saddle-node periodic orbit p with zero strong unstable dimension; see figure 7.1. This is a codimension one generic situation. Breaking p into a pair of hyperbolic periodic orbits, the vector field becomes Morse-Smale, locally near the original homoclinic loop: a finite number of periodic orbits (here: two), all hyperbolic, with transverse intersections of their stable/unstable manifolds. Perturbing into the opposite direction, a strange attractor of fractal dimension appears; for estimates and more details see [Afraimovich & Shereshevsky] (1991). Introducing a second parameter, we may consider $\tilde{h}$ hitting a two-dimensionally unstable hyperbolic saddle A, thus forming a heteroclinic loop between an equilibrium and a periodic saddle-node; see figure 7.1. Perturbing such that the periodic saddle-node disappears, we will also find a path γ of homoclinic orbits with associated

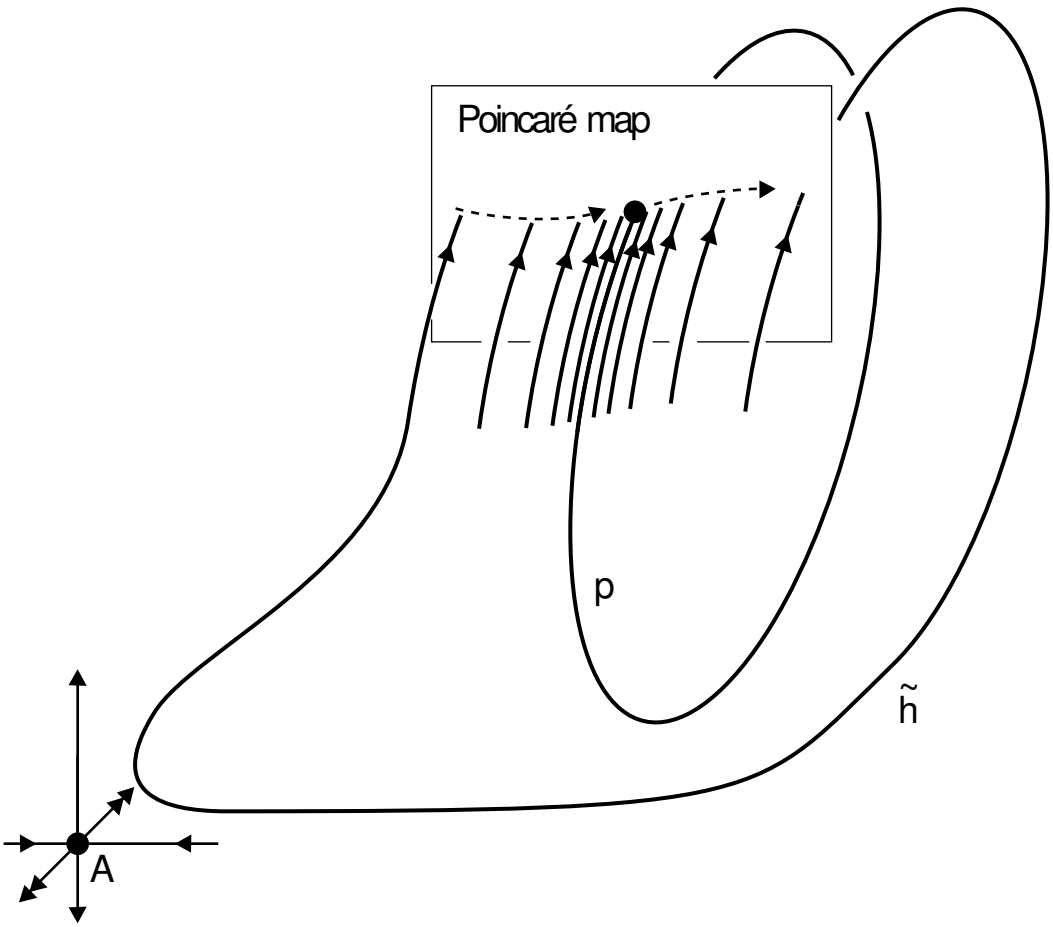

Figure 7.1: Generating a het loop between an equilibrium and a periodic saddle-node.

equilibrium near A. Clearly ϵ-length blows up, as γ approaches the periodic saddle-node. Recall that typically a strange attractor of fractal dimension appears near termination of the A-hom path. Summarizing, each case of theorem 3.4 may in fact occur.

Theorem 3.4, as it stands, is formulated only for finite-dimensional flows. For infinite-dimensional dynamical systems, results are available concerning the transition from homoclinic to periodic orbits, and time periodic forcing of homoclinic orbits. Using the methods of [Lin] (1990), for example, it is fairly clear that typical homoclinic orbits will again be accompanied by a sheet of periodic orbits just as in the finite-dimensional case. For the contractive case see also [Chow & Deng] (1987). Index theories for periodic orbits and their bifurcations are readily available, along with a notion of genericity, see for example [Chow & Mallet-Paret] (1978), [Fiedler] (1985, 1986 b). So far, however, a two-parameter homoclinic bifurcation result has not been established, to our knowledge; not even for reaction diffusion systems or delay equations. Due to compactness of the semiflows, we claim that theorem 3.4, together with remark 3.5 (iii), carries over to the infinite-dimensional settings used in the above references. Note, however, that our list of sample bifurcations collapses entirely, strictly speaking, in the infinite-dimensional case. In particular, our notions of stratified versus non-stratified loops are not yet founded on ample evidence. For promising techniques, especially for delay equations, we mention [Lin] (1990) and [Walther] (1989).

For Volterra type integral equations, the situation is even more hazy. In [Fiedler] (1986 a) a global Hopf bifurcation result was proved, by finite-dimensional ODE approximation. But our present results on homoclinic continuation critically depend on our genericity assumptions which, of course, need not survive an approximation process. We will return to this genericity question below.

Numerical pathfollowing of periodic orbits for one-parameter flows has become standard, by now. See e.g. [Doedel & Kernevez] (1985), [Khibnik et al.] (1992), [Kubiček & Marek] (1983), [Rheinboldt] (1983), [Seydel] (1988). For the analogous problem of numerical pathfollowing of homoclinic orbits for two-parameter flows, there are only relatively few results available; for a line of research see [de Hoog & Weiss] (1979), [Lentini & Keller] (1980), [Beyn] (1990), [Doedel & Friedman] (1992), [Kuznetsov] (1990). To our knowledge, a systematic homoclinic pathfollowing code is not yet available. In particular, we are not aware of any systematic numerical approach to homoclinic bifurcations.

Taking a somewhat simplistic view point, time discretization might be considered as an approximation of a continuous time dynamical system by discrete time dynamics. In particular, even tame homoclinic orbits should in principle be considered as transverse, numerically. It turns out that the transversality effects, and the related Smale horseshoe shift dynamics, are exponentially small in the discretization step size; see [Fiedler & Scheurle] (1991). Although we may therefore safely neglect the accompanying transversality effects as "spurious", in most cases of practical interest, these effects may cause problems at exponentially flat homoclinic bifurcations such as resonant homoclinic doubling, see example 2.9 and [Chow et al.] (1990 a). It is particularly in such numerically rather delicate situations where we expect theorem 3.4 and its proof to help. Indeed, we might choose to avoid the intricate tangles of discrete time analogues of our homoclinic bifurcations. Instead, we could isolate the suspected singularity by a surrounding circle S, in parameter space. The proof in section 4 then suggests to follow paths of periodic orbits along such a circumventing circle S and match pairs of tame hom paths, according to our index theory, without ever touching the messy interior of S. There is no need to ever determine precisely what type of ho-

moclinic bifurcation the circle S circumvents, as long as it is stratified. The only one-parameter homoclinic "bifurcation" which has to be understood well then, numerically, is that of periodic orbits limiting onto a tame homoclinic orbit. Unlike poor Laokoon, we should faithfully follow the periodic snakes along S, rather than fighting against them. This way we can avoid getting entangled too much in our pathfollowing attempts. Because our theoretical results are of a global nature, the diameter of the circle S is not a critical quantity. For example, the diameter of S need not be comparable to the size of a single, small numerical hom pathfollowing step. Of course, the interior of S will remain a white spot in the bifurcation diagram unless the homoclinic orbits are traced further inward. We realize that it is a long way from the above remarks to a fully implemented efficient algorithm. Still, we hope that such an algorithm will appear, tracing out the alternatives of theorem 3.4 in specific applied context.

One popular approach to homoclinic orbits $h(t)$ is to view them as solutions of a problem

$$\frac{d}{dt}x(\cdot) - f(\lambda, x(\cdot)) = 0 \tag{7.1}$$

with $x(\cdot) \in \mathfrak{X}$, a suitable Banach space of X-valued functions on the real line, $t \in \mathbb{R}$, for example $\mathfrak{X} = BC^0(\mathbb{R}, X)$ or $BC^1(\mathbb{R}, X)$ with sup norms. In other words, (7.1) is a boundary value problem on the whole real line, and the space $\mathfrak{X}$ imposes boundary conditions "at infinity". Under exponential dichotomy assumptions, the linearization with respect to $x(\cdot)$ becomes a Fredholm operator, [Palmer] (1984), and local continuation via implicit function theorem applies, [Chow & Hale] (1982). Numerical discretization of $h(t)$ can be treated in the same spirit, by adding a time periodic perturbation $\epsilon^p g(\epsilon, \lambda, t/\epsilon, x(\cdot))$ with amplitude ϵ^p and time period ϵ determined by numerical order p and step size ϵ; see [Fiedler & Scheurle] (1991). Inverting $\frac{d}{dt}$ in $\mathfrak{X}$, and rewriting (7.1) as

$$x(\cdot) - (\tfrac{d}{dt})^{-1} f(\lambda, x(\cdot)) = 0, \tag{7.2}$$

Leray-Schauder degree can be applied since (7.2) is a compact perturbation of identity. For the technically much more demanding problem of solitary water waves and elliptic partial differential equations in unbounded strips this idea has been pursued in [Amick & Kirchgässner] (1989).

Global bifurcation of periodic orbits has successfully been treated in a similar boundary value problem setting, with $\mathfrak{X}$ carrying periodic boundary conditions and period scaled out as an explicit parameter. See for example [Ize] (1976). More recent variants, [Dyławerski et al.] (1991), [Gęba et al.] (1991), [Ize et al.] (1989, 1991), make explicit use of advanced topology and of $SO(2)$-equivariance of (7.1), (7.2) with respect to time shift.

We did not favor the boundary value problem approach, here, because it is intrinsically inadequate to treat most homoclinic or heteroclinic bifurcations. Consider resonant homoclinic doubling, 2.9, for example. Although the 2-hom branch converges to the 1-hom branch (traced out twice), in phase space $\Lambda \times X$ and at bifurcation, the corresponding profiles will not converge in $\mathfrak{X}$, be it a C^k-, a Hölder-, or a Sobolev space. Following the 1-hom path, the 2-hom path remains far away in these topologies. Approaching the bifurcation along the 2-hom path, a limiting profile need not exist. Our notion of homoclinic continuation through a stratified loop just cannot be expressed in terms of any such space $\mathfrak{X}$.

Our results crucially hinge on a genericity assumption for the vector field $f(\lambda, x)$. By genericity, we have B-points as starting points of homoclinic pathfollowing. By genericity, we obtain the sheet of periodic orbits which accompanies hom paths. Also the validity of the concept of isolated, codimension two stratified loops is critically tied to this assumption, as are all our examples of homoclinic bifurcation. When additional structure of the

equations is known, there are two basic ways to incorporate this information. First, we can aim for a result which survives the limiting process of generic systems approximating non-generic ones. For example, Brouwer degree $\deg(f, \Omega, y)$ may first be defined for regular values y of f on Ω; in a second step arbitrary y are approximated by regular values. For examples on global Hopf bifurcation involving approximations $p_n(\cdot) \to p(\cdot)$ of periodic orbits p see [Fiedler] (1985, 1986 b, 1988) and the references there. This approximation can be understood in terms of "virtual periods", see definition 2.11 above. Recall that virtual periods provide a necessary criterion for bifurcations: limits of minimal periods of $p_n(\cdot)$ are virtual periods of the limit $p(\cdot)$. When the ultimate goal is a universal result which survives the approximation process, only density of generic sets is used. In particular, genericity is then as appropriate a concept as "prevalence", introduced in [Hunt et al.] (1991), or any other approximation process. Unfortunately, however, a tool analogous to virtual periods is still missing, for homoclinic orbits.

The second way to incorporate additional structure of the underlying equations is by simultaneously restricting the notion of genericity: consider open dense subsets within the particular class of vector fields under consideration. The two basic ingredients which we then need for our pathfollowing approach are the following:

(7.3.a) transition from homoclinic to periodic orbits, and

(7.3.b) an index theory for periodic orbits,

each in the appropriate structural context. Specifically we comment on equivariance, reversibility, and Hamiltonian structure next.

Consider equivariant vector fields f, e.g. $X = \mathbb{R}^N$ and f commutes with a compact Lie group G acting linearly on $X = \mathbb{R}^N$,

(7.4) $$f(\lambda, gx) = gf(\lambda, x),$$

for all $g \in G, (\lambda, x) \in \Lambda \times X$. In particular, $t \to gx(t)$ is a time trajectory if, and only if, $x(t)$ is; for example $x(t)$ could be stationary, periodic, homoclinic, or heteroclinic. An index theory in the spirit of definition 3.1 is available for periodic orbits in the presence of equivariance, see [Fiedler] (1988). The relevant groups here are cyclic factors in G. A two-parameter extension including B-points has not yet been developed.

Accounting for the transition (7.3.a) from homoclinic to periodic orbits, in a systematic equivariant way, is also a somewhat involved problem; see for example [Armbruster et al.] (1988), [Krupa & Melbourne] (1991), [Chossat] (1992), [Scheel & Chossat] (1992), and the references there. To sketch the basic problem, consider a homoclinic trajectory $x = h(t)$ with associated equilibrium A. Let $G_A \supseteq G_h$ denote the respective subgroups of elements in G fixing $A, h(t)$ pointwise. We may work in the linear, flow invariant subspace $Fix(G_h)$ of vectors in X which are fixed under G_h. If $G_h = G_A$, then the standard transition from homoclinic to periodic trajectories works well in $Fix(G_h)$. Next suppose G_h is strictly contained in G_A and, for simplicity, G_h is a normal subgroup of G_A. Then G_A acts on $Fix(G_h)$ and maps $h(t)$ to several copies, all homoclinic to A. A "trivial" caveat is the Lorenz explosion where $G = G_A = \mathbb{Z}_2$ and $G_h = id$.

Widening the notion of homoclinicity somewhat, we may require $h(t)$ to just be heteroclinic from A to another equilibrium B, but with $B = gA$ in the same group orbit as A. Assume, again for simplicity, that G_A is a normal subgroup of G and the factor group G/G_A of order $|G/G_A|$ is finite cyclic, generated by gG_A. Then, acting with G on A and h gives rise to a heteroclinic loop composed of $|G/G_A|$ copies of h. In a non-equivariant generic setting it requires $|G/G_A|$ parameters to unfold such a loop. In contrast, such a loop can be codimension one, or even structurally stable, within the equivariant category. Again, it can be a challenging problem in itself to analyze the

nearby periodic trajectories and their symmetries. Specific examples are discussed in the above references. Although the combined complexity of symmetry breaking and homoclinic bifurcation may seem overwhelming, we still believe that our approach can be helpful at least in some particular cases, say with cyclic symmetries. Also our original approach is particularly suitable for forced symmetry breaking, where the full equivariance is assumed to hold only at an isolated point $\lambda = 0$ in two-parameter space.

Time reversibility is a somewhat more subtle "symmetry" constraint. Let R be a linear involution on X; for example suppose R fixes the first N components on $X = \mathbb{R}^{2N}$ and reverses the signs of the remaining N components. Time reversibility means that

$$f(\lambda, Rx) = -Rf(\lambda, x), \tag{7.5}$$

for all $(\lambda, x) \in \Lambda \times X$. Second order systems

$$\ddot{q} + v(\lambda, q) = 0, \qquad q \in \mathbb{R}^N \tag{7.6}$$

provide an example with $R(q, \dot{q}) = (q, -\dot{q})$. In general $x(t)$ is a solution if, and only if, $Rx(-t)$ is. Thus reversibility imposes a constraint on those trajectories which are invariant under R, as a set. Equivalently, these are the trajectories intersecting $Fix(R)$. Call such trajectories *symmetric*. It was observed by [Devaney] (1977) that symmetric homoclinic orbits are typically persistent under reversible perturbations, and are accompanied by a one-parameter family of likewise symmetric periodic orbits; see also the account in [Vanderbauwhede & Fiedler] (1992). Of course, the associated equilibrium A must lie in $Fix(R)$, and the linearization at A therefore defines a linear reversible vector field. In particular, the spectrum is point symmetric with respect to 0 in $\mathbb{C}$, and hence also with respect to reflection at the imaginary axis. Therefore, resonance conditions for the principal eigenvalues $\mu_\pm$ are automatic:

(7.7) $\qquad Re\mu_+ + Re\mu_- = 0,$

in contrast to nonresonance conditions (2.4.a,b) for tame homoclinic orbits; see also our (non-reversible) resonance example 2.9. For real $\mu_\pm$, some homoclinic bifurcations involving symmetric A have been discussed in [Perouème] (1991). One interesting example involves a family of symmetric periodic orbits limiting onto a figure 8 symmetric pair of non-symmetric homoclinic orbits with the same, symmetric associated equilibrium A. The case of complex $\mu_\pm$ seems largely open; but shift dynamics is known to occur in the related Hamiltonian case [Devaney] (1976). An additional complication arises since purely imaginary eigenvalues at A cannot be perturbed to have nonzero real parts, due to symmetry of the spectrum. Again, associated homoclinic orbits with shift dynamics have been analyzed in the Hamiltonian but not in the reversible case; see [Holmes et al.] (1992). Global pathfollowing has not yet been attempted.

The Hamiltonian case, for example

(7.8) $\qquad \dot{x} = J \operatorname{grad}_x H, \qquad J = \begin{pmatrix} 0 & id \\ -id & 0 \end{pmatrix},$

$x = (q,p) \in X = \mathbb{R}^{2N}$, has been studied quite extensively, at least as far as time periodic solutions are concerned. The reversible second order system (7.6) is a specific example, if we assume $v = \operatorname{grad}_q V$ is a gradient, $H(p,q) = p^2/2 + V(q)$. For surveys see, for example, [Ekeland] (1990), [Rabinowitz] (1986), [Mawhin & Willem] (1989), [Struwe] (1990), and the references there. Fairly recently homoclinic orbits are receiving increased attention, mostly in the autonomous and periodically forced case; see, e.g., [Angenent] (1992), [Coti Zelati et al.] (1990), [Coti Zelati & Rabinowitz] (1990, 1991), [Hofer& Wysocki] (1990). All these results are based on variational methods, alias least action principles. Notably, the possibility of homoclinic bifurcation is related to failure of the Palais-Smale compactness

condition. Continuation of solutions is traditionally not considered, perhaps because minimizers need not vary continuously with parameters (but critical points do). Avoiding the variational setting, [Alexander & Yorke] (1978) use a one-parameter dissipative embedding

$$\dot{x} = J \operatorname{grad}_x H + \nu \operatorname{grad}_x H, \quad \nu \in \mathbb{R}, \tag{7.9}$$

to utilize one-parameter results on global Hopf bifurcation for Hamiltonian systems. Indeed, periodic solutions can occur only for $\nu = 0$ because, for $\nu \neq 0$, H serves as a Lyapunov functional. In this way, two-parameter results on homoclinic continuation should provide one-parameter results for Hamiltonian systems or, more generally, for systems with a first integral H. As we have mentioned above, we are unfortunately lacking a concept like virtual periods which would survive an approximation of the dissipative embedding (7.9) by generic vector fields. It may be interesting to note that the ingredients (7.3 a,b) to the alternative approach, genericity within the class of Hamiltonian systems, are available: see [Vanderbauwhede & Fiedler] (1992) for the transition homoclinic to periodic, and [Mallet-Paret & Yorke] (1982) for a Hamiltonian orbit index. Still a pathfollowing approach in the present spirit will probably be limited to real principal eigenvalues, due to the shift dynamics results by [Devaney] (1976) and [Holmes et al.] (1992) mentioned above.

Typical spaces $\mathfrak{X}$ for homoclinic orbits $h(\cdot)$ in a variational Hamiltonian context are L^p- and $W^{1/2}$-spaces, similarly to the boundary value problems sketched above. Measuring the length of $h(\cdot)$ corresponds, of course, to a $W^{1,1}$-norm. In contrast, ϵ-length is somewhat like a $W^{1,1}_{loc}$-topology, as long as only one associated equilibrium A is involved and an appropriate parametrization is chosen for $h(\cdot)$. For heteroclinic loops, this analogy fails. A very interesting non-local matching construction, which overcomes the boundary value problem topology obstacle and resembles shadowing ideas in dynamical

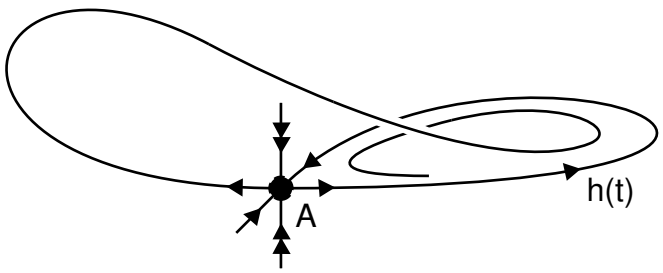

Figure 7.2: An orbit which is heteroclinic from A to an A-hom orbit; [Homburg] (1992).

systems, was presented by [Coti Zelati & Rabinowitz] (1990). In fact, shift type dynamics near transverse homoclinic points is imitated in a variational context. This allows generalization to elliptic equations in several unbounded space dimensions which originally lack a dynamical systems interpretation; see [Coti Zelati & Rabinowitz] (1991).

In figure 7.1, we have indicated one way how ϵ-length might become unbounded along a bounded hom path. That mechanism was related to the hom path approaching the boundary $\mathfrak{B}$ of the closure of the set of Morse-Smale systems. Also, Belyakov transitions 5.4 lie on $\mathfrak{B}$, at least locally, and chaotic homoclinic orbits lie beyond. Here "beyond" means "outside the closure of the set of Morse-Smale systems". Generic folds with a least two associated homoclinic orbits also lie beyond $\mathfrak{B}$, recalling example 5.1. Consider a non-stratified loop H in the sense of proposition 2.8 and definition 2.11 next. Suppose H cannot be perturbed to become stratified. Then H (or, in fact, the vector field belonging to H) lies on $\mathfrak{B}$ or beyond. On the other hand, stratified loops may also lie on $\mathfrak{B}$, or beyond. Even tame homoclinic orbits may. An example considered by [Homburg] (1992) is sketched in figure 7.2. It involves a dissipative saddle A on an invariant 2-manifold

with a homoclinic orbit h, attractive from "inside". The other half of the unstable manifold of A is then fed back to the "inside" of h, accumulating onto clos(h) for $t \to +\infty$. This situation corresponds to an A-to-periodic heteroclinic orbit, when the periodic orbit has just become homoclinic to A. For simplicity we assume A to be only one-dimensionally unstable. We consider only the case where the limiting A-to-h heteroclinic orbit is non-twisted; the bifurcation can then be realized by vector fields on a 2-torus embedded e.g. in $\mathbb{R}^3$. Again, such a system is on the Morse-Smale boundary $\mathfrak{B}$. As long as the periodic orbit associated to h exists, that orbit is an attractor and the system is Morse-Smale with two A-to-periodic heteroclinic orbits. After the periodic orbit has dissolved via h, however, the dynamics can be described by a discontinuous one-dimensional map. Phenomena like intermittency, Cantor type bifurcation sets, and renormalization structures arise. The homoclinic orbit h itself, however, is tame according to our definitions. It is not the pathfollowing of h, which causes problems here, but pathfollowing of the infinity of homoclinic orbits which start out opposite to h, for $t \to -\infty$, and re-settle into A only after n revolutions along h, $n \geq n_0$ any large integer.

It is these intricacies which make our pathfollowing attempt inadequate, unsatisfactory, and incomplete. On the one hand, it seems quite easy to probe into the labyrinth of chaotic complexity along a homoclinic path, at least for a while. On the other hand, once inside, there is no visible Ariadne thread to help us move around. The above example shows that, while following h, we may in fact have already entered the labyrinth without being much aware of it. Tresser's non-stratified figure 8, composed of two separately tame homoclinic orbits, is another such case; see 2.10 and figure 2.7. It is even quite feasible, in that case, to choose arbitrarily small circles S in Λ around the figure 8 parameter value $\lambda = \lambda_0$, such that S "sees" only finitely many homs

and attached per branches. In particular, pathfollowing would be possible, matching hom paths along S as in section 4. The interior of S then remains a "white spot" in the global bifurcation diagram. Unfortunately, adopting such a strategy, we may inadvertently have to remove countably many discs – effectively wiping out major parts of the bifurcation diagram. Before we will be able to do better than that, we will need a deeper understanding of that tremendously rich zoo of homoclinic and heteroclinic bifurcations.

Quoting [Poincaré, p. 82] (1892) in the translation by [Ekeland] (1990), periodic solutions appear " ...to be the only opening through which we can force our way into an otherwise impenetrable citadel ...". Extending to homoclinic orbits, we have still largely followed Poincaré's advice. The present paper is not much more than a feeble attempt to detect order in the complexities ruling homoclinic orbits. We have, in other words, investigated the homoclinic part of the large period limit of periodic orbits. Introducing terminology like "stratified loops" is a risk. It is not clear, at present, whether or not such a notion will be the most appropriate. Mainly, we are still lacking a sufficient catalogue of examples. But there is some consolation, too. In the future, more and more examples will enter the homoclinic bifurcation catalogue. Among them, some ought to be stratified. This will only widen the scope of the results presented here. Hopefully, *you* will contribute ...

References

R. Abraham & J. Robbin. *Transversal Mappings and Flows.* Benjamin Inc., Amsterdam, 1967.

V. S. Afraimovich & M. A. Shereshevsky. The Hausdorff dimension of attractors appearing by saddle-node bifurcations. Int. J. Bif. Chaos **1** (1991), 309–325.

V. S. Afraimovich & L. P. Shilnikov. On attainable transitions from Morse-Smale systems to systems with many periodic points. Math. USSR Izvestija **8** (1974), 1235–1270.

J. C. Alexander & J. A. Yorke. Global bifurcation of periodic orbits. Amer. J. Math. **100** (1978), 263–292.

C. J. Amick & K. Kirchgässner. A theory of solitary water waves in the presence of surface tension. Arch. Rat. Mech. Anal. **105** (1989), 1–49.

S. Angenent. A variational interpretation of Melnikov's function and exponentially small separatrix splitting. Preprint, 1992.

D. Armbruster & J. Guckenheimer & P. Holmes. Heteroclinic cycles and modulated travelling waves in systems with $O(2)$ symmetry. Physica D **29** (1988), 257–282.

V. I. Arnol'd. Lectures on bifurcations and versal systems. Russ. Math. Surv. **27** (1972), 54–123.

V. I. Arnol'd. *Geometrical Methods in the Theory of Ordinary Differential Equations.* Springer-Verlag, New York, 1983.

V. I. Arnol'd (ed.). *Dynamical Systems V. Theory of Bifurcations and Catastrophes.* Enc. Math. Sciences **5**, Springer-Verlag, Berlin, 1992.

L. A. Belyakov. Bifurcation set in a system with homoclinic saddle curve. Mat. Zam. **28** (1980), 911–922.

L. A. Belyakov. Bifurcation of systems with homoclinic curve of a saddle-focus with saddle quantity zero. Mat. Zam. **36** (1984), 838–843.

W.-J. Beyn. The numerical computation of connecting orbits in dynamical systems. IMA Z. Numer. Anal. **9** (1990), 379–405.

R. Bogdanov. Bifurcation of the limit cycle of a family of plane vector fields. Russ. (1976), Engl.: Sel. Mat. Sov. **1** (1981), 373–387.

R. Bogdanov. Versal deformations of a singularity of a vector field on the plane in the case of zero eigenvalues. Russ. (1976), Engl.: Sel. Mat. Sov. **1** (1981), 389–421.

V. V. Bykov. On the structure of a neighborhood of a separatrix contour with a saddle-focus (Russ.). Methods Qual. Th. Diff. Eq. **133** (Gorki, 1978), 3–32.

V. V. Bykov. On bifurcations of dynamical systems which are close to systems with a separatrix contour (Russ.). Methods Qual. Th. Diff. Eq. **224** (Gorki, 1980), 44–72.

V. V. Bykov. On nontrivial hyperbolic sets arising from a contour which consists of saddle separatrices (Russ.). Methods Qual. Bifurcation Th. **120** (Gorki, 1988), 22–32.

P. Chossat. Forced reflectional symmetry breaking of an $O(2)$-symmetric homoclinic cycle. Preprint, 1992.

S.-N. Chow & B. Deng. Bifurcation of a unique periodic orbit from a homoclinic orbit in infinite-dimensional systems. Trans. Amer. Math. Soc. **312** (1989), 539–587.

S.-N. Chow & B. Deng & B. Fiedler. Homoclinic bifurcation at resonant eigenvalues. J. Dyn. Diff. Eq. **2** (1990), 177–244.

S.-N. Chow & B. Deng & D. Terman. The bifurcation of a homoclinic orbit and periodic orbits from two heteroclinic orbits. SIAM J. Math. Anal. **21** (1990), 179–204.

S.-N. Chow & B. Deng & D. Terman. The bifurcation of a homoclinic orbit from two heteroclinic orbits – a topological approach. Applic. Analysis **42** (1991), 275–300.

S.-N. Chow & J. K. Hale. *Methods of Bifurcation Theory.* Springer-Verlag, New York, 1982.

S.-N. Chow & X.-B. Lin. Bifurcation of a homoclinic orbit with a saddle-node equilibrium. Diff. Integr. Eq. **3** (1990), 435–466.

S.-N. Chow & J. Mallet-Paret. The Fuller index and global Hopf bifurcation. J. Diff. Eq. **29** (1978), 66–85.

S.-N. Chow & J. Mallet-Paret & J. Yorke. A periodic orbit index which is a bifurcation invariant. In [Palis](1983), 109–131.

C. C. Conley. *Isolated Invariant Sets and the Morse Index.* CBMS Notes **38**, AMS, Providence, 1978.

V. Coti Zelati & I. Ekeland & E. Séré. A variational approach to homoclinic orbits in Hamiltonian systems. Math. Ann **288** (1990), 133–160.

V. Coti Zelati & P. H. Rabinowitz. Homoclinic orbits for second order Hamiltonian systems possessing superquadratic potentials. Preprint, 1990.

V. Coti Zelati & P. H. Rabinowitz. Homoclinic type solutions for a semilinear elliptic PDE on $\mathbb{R}^n$. Preprint, 1991.

B. Deng. Homoclinic bifurcations with nonhyperbolic equilibria. SIAM J. Math. Anal. **21** (1990), 693–720.

B. Deng. The bifurcations of countable connections from a twisted heteroclinic loop. SIAM J. Math. Anal. **22** (1991), 653–679.

B. Deng. The existence of infinitely many travelling front and back waves in the FitzHugh-Nagumo equations. SIAM J. Math. Anal. **22** (1991), 1631–1650.

R. Devaney. Homoclinic orbits in Hamiltonian systems. J. Diff. Eq. **21** (1976), 431–438.

R. Devaney. Blue sky catastrophes in reversible and Hamiltonian systems. Ind. Univ. Math. J. **26** (1977), 247–263.

E. J. Doedel & M. J. Friedman. Numerical computation of heteroclinic orbits. J. Comp. Appl. Math., to appear 1992.

E. J. Doedel & J. P. Kernevez. Software for continuation problems in ordinary differential equations with applications. CALTECH 1985.

F. Dumortier & R. Roussarie & J. Sotomayor & H. Żoładek *Bifurcations of Planar Vector Fields.* Springer-Verlag, Berlin 1991.

G. Dyławerski & K. Gęba & J. Jodel & W. Marzantowicz. S^1-equivariant degree and the Fuller index. Ann. Pol. Math. **52** (1991), 243–280.

I. Ekeland. *Convexity Methods in Hamiltonian Mechanics.* Springer-Verlag, Berlin, 1990.

J. Evans & N. Fenichel & J. A. Feroe. Double impulse solutions in nerve axon equations. SIAM J. Appl. Math. **42** (1982), 219–234.

J. A. Feroe. Existence and stability of multiple impulse solutions of a nerve axon equation. SIAM J. Appl. Math. **42** (1982), 235–246.

B. Fiedler. An index for global Hopf bifurcation in parabolic systems. J. reine angew. Math. **359** (1985), 1–36.

B. Fiedler. Global Hopf bifurcation for Volterra integral equations. SIAM J. Math. Anal. **17** (1986), 911–932.

B. Fiedler. Global Hopf bifurcation of two-parameter flows. Arch. Rat. Mech. Anal. **94** (1986), 59–81.

B. Fiedler. *Global Bifurcation of Periodic Solutions with Symmetry.* Springer-Verlag, Berlin, 1988.

B. Fiedler & J. Scheurle. Discretization of homoclinic orbits and invisible chaos. Preprint, 1991.

J.-M. Gambaudo. *Ordre, désordre, et frontière des systèmes Morse-Smale.* These, Nice, 1987.

K. Gęba & W. Krawcewicz & J. Wu. An equivariant degree with applications to symmetric bifurcation problems 1: construction of the degree. Preprint, 1991.

J. Guckenheimer & P. Holmes. *Nonlinear Oscillations, Dynamical Systems, and Bifurcations of Vector Fields.* Springer-Verlag, New York, 1990.

J. K. Hale. *Asymptotic Behavior of Dissipative Systems.* Math. Surv. **25**, AMS, Providence 1988.

J. Harrison. C^2 counterexamples to the Seifert conjecture. Topology **27** (1988), 249–278.

J. Harrison & J. A. Yorke. Flows on S^3 and $\mathbb{R}^3$ without periodic orbits. In [Palis](1983), 401–407.

S. P. Hastings. Single and multiple pulse waves for the FitzHugh-Nagumo equations. SIAM J. Appl. Math. **42** (1982), 247–260.

M. W. Hirsch. *Differential Topology.* Springer-Verlag, New York, 1976.

H. Hofer & K. Wysocki. First order elliptic systems and the existence of homoclinic orbits in Hamiltonian systems. Preprint, 1990.

P. J. Holmes & A. Mielke & O. O'Reilly. Cascades of homoclinic orbits to, and chaos near, a Hamiltonian saddle-center. J. Dyn. Diff. Eq. **4** (1992), 95–126.

A. J. Homburg. Bifurcations of saddle-saddle type homoclinic orbits in vector fields. Preprint 1992.

P. de Hoog & R. Weiss. The numerical solution of boundary value problems with an essential singularity. SIAM J. Numer. Anal. **16** (1979), 637–669.

B. R. Hunt & T. Sauer & J. A. Yorke. Prevalence: a translation invariant "almost everywhere" on infinite dimensional spaces. Preprint, 1991.

J. Ize. *Bifurcation Theory for Fredholm Operators.* AMS memoir **174**, Providence, 1976.

J. Ize & I. Massabò & V. Vignoli. Degree theory for equivariant maps I. Trans. AMS **315** (1989), 433–510.

J. Ize & I. Massabò & V. Vignoli. Degree theory for equivariant maps: the general S^1-action. Preprint, 1991.

A. I. Khibnik & Y. A. Kuznetsov & V. V. Levitin & E. V. Nikolaev. Continuation techniques and iterative software for bifurcation analysis of ODEs and iterated maps. Physica D, to appear 1992.

M. Kisaka & H. Kokubu & H. Oka. Bifurcations to n-homoclinic orbits and n-periodic orbits in vector fields. Preprint, 1992.

H. Kokubu. Homoclinic and heteroclinic bifurcations of vector fields. Japan J. Appl. Math. **5** (1988), 455–501.

H. Kokubu. Heteroclinic bifurcations associated with different saddle indices. Preprint, 1990.

H. Kokubu. A construction of three dimensional vector fields which have a codimension two heteroclinic loop at Glendinning-Sparrow T-point. Preprint, 1991.

M. Krupa & I. Melbourne. Asymptotic stability of heteroclinic cycles in systems with symmetry. Preprint, 1991.

M. Kubiček & M. Marek. *Computational Methods in Bifurcation Theory and Dissipative Structures*. Springer-Verlag, New York, 1983.

Y. A. Kuznetsov. Computation of invariant manifold bifurcations. In D. Roose et al., eds., *Continuation and Bifurcations: Numerical Techniques and Applications*, 183–195. Kluwer, Netherlands, 1990.

M. Lentini & H. B. Keller. Boundary value problems on semi-infinite intervals and their numerical solution. SIAM J. Numer. Anal. **17** (1980), 577–604.

E. Leontovich. On the generation of limit cycles from separatrices (Russ.). Dokl. Akad. Nauk **78** (1951), 641–644.

X.-B. Lin. Using Melnikov's method to solve Shilnikov's problems. Proc. Roy. Soc. Edinburgh **116A** (1990), 295–325.

V. I. Lukyanov. Bifurcations of dynamical systems with a saddle-node separatrix loop. Diff Eq. **18** (1982), 1049–1059.

J. Mallet-Paret & J. A. Yorke. Snakes: oriented families of periodic orbits, their sources, sinks, and continuation. J. Diff. Eq. **43** (1982), 419–450.

J. Mawhin & M. Willem. *Critical Point Theory and Hamiltonian Systems.* Springer-Verlag, New York, 1989.

M. Medved. The unfoldings of a germ of vector fields in the plane with a singularity of codimension 3. Czech. Math. J. **35** (1985), 1–42.

J. Palis, jr., ed. *Geometric Dynamics.* Springer-Verlag, New York, 1983.

K. J. Palmer. Exponential dichotomies and transversal homoclinic points. J. Diff. Eq. **55** (1984), 225–256.

M.-C. Perouéme. Bifurcations d'orbites homoclines dans les systèmes reversibles. Thesis, Nice 1992.

H. Poincaré. *Méthodes Nouvelles de la Mécanique Céleste I.* Gauthiers-Villars, Paris, 1892.

P. H. Rabinowitz. *Minimax Methods in Critical Point Theory with Applications to Differential Equations.* CBMS Notes **65**, AMS, Providence, 1986.

W. C. Rheinboldt & J. W. Burkardt. A locally parametrized continuation process. ACM Trans. Math. Software **9** (1983), 215–235.

C. Robinson. Differentiability of the stable foliation for the model Lorenz equations. In D. Rand & L. Young, eds., *Dynamical Systems and Turbulence.* Springer-Verlag, Berlin, 1981.

B. Sandstede. Personal communication. 1992.

S. Schecter. The saddle-node separatrix-loop bifurcation. SIAM J. Math. Anal. **18** (1987), 1142–1156.

S. Schecter. Melnikov's method at a saddle-node and the dynamics of a forced Josephson junction. SIAM J. Math. Anal. **18** (1987), 1699–1715.

A. Scheel & P. Chossat. Bifurcation d'orbites périodiques à partir d'un cycle homocline symétrique. C. R. Acad. Sci. Paris, Ser. I **314** (1992), 49–54.

P. A. Schweitzer. Counterexamples to the Seifert conjecture and opening closed leaves of foliations. Ann. of Math. **100** (1974), 386–400.

R. Seydel. *From Equilibrium to Chaos.* Elsevier, New York, 1988.

L. P. Shilnikov. Some cases of generation of periodic motions in an n-dimensional space. Soviet Math. Dokl. **3** (1962), 394–397.

L. P. Shilnikov. A case of the existence of a countable number of periodic motions. Soviet Math. Dokl. **6** (1965), 163–166.

L. P. Shilnikov. On the generation of a periodic motion from a trajectory which leaves and re-enters a saddle-saddle state of equilibrium. Soviet Math. Dokl. **7** (1966), 1155–1158.

L. P. Shilnikov. The existence of a denumerable set of periodic motions in four-dimensional space in an extended neighborhood of a saddle-focus. Soviet Math. Dokl. **8** (1967), 54–57.

L. P. Shilnikov. On the generation of a periodic motion from trajectories doubly asymptotic to an equilibrium state of saddle type. Math. USSR Sbornik **6** (1968), 427–437.

L. P. Shilnikov. On a new type of bifurcation of multidimensional dynamical systems. Soviet Math. Dokl. **10** (1969), 1368–1371.

L. P. Shilnikov. A contribution to the problem of the structure of an extended neighborhood of a rough equilibrium state of saddle-focus type. Math. USSR Sbornik **10** (1970), 91–102.

C. Sparrow. *The Lorenz Equations: Bifurcations, Chaos, and Strange Attractors.* Springer-Verlag, New York, 1982.

M. Struwe. *Variational Methods.* Springer-Verlag, Berlin, 1990.

F. Takens. Singularities of vector fields. Publ. IHES **43** (1974), 47–100.

C. Tresser. About some theorems by L.P. Shilnikov. Ann. Inst. H. Poincaré **40** (1984), 441–461.

A. Vanderbauwhede & B. Fiedler. Homoclinic period blow-up in reversible and conservative systems. Z. angew. Math. Phys. **43** (1992), 292–318.

H.-O. Walther. *Hyperbolic periodic solutions, heteroclinic connections and transversal homoclinic points in autonomous differential delay equations.* AMS memoir **402**. AMS, Providence, 1989.

G. T. Whyburn. *Topological Analysis.* Princeton Univ. Press, Princeton, 1968.

S. Wiggins. *Global Bifurcations and Chaos – Analytical Methods.* Springer-Verlag, New York, 1988.

E. Yanagida. Branching of double pulse solutions from single pulse solutions in nerve axon equations. J. Diff. Eq. **66** (1987), 243–262.